Biosensors and Bioelectronics: X 18 (2024) 100478

Contents lists available at ScienceDirect

Biosensors and Bioelectronics: X

journal homepage: www.journals.elsevier.com/biosensors-and-bioelectronics-x

Biosensors for amplification-free viral RNA detection

Brenda G. Parassol [a], Nayla Naomi Kusimoto Takeuti [b], Henrique Antonio Mendonça Faria [c], Kelly C. Jorge [a], Isabella Sampaio [b], Valtencir Zucolotto [b], Nirton C.S. Vieira [a,*]

[a] Institute of Science and Technology, Federal University of São Paulo, 12231-280, São José dos Campos, SP, Brazil
[b] Nanomedicine and Nanotoxicology Group, Physics Institute of São Carlos, University of São Paulo, CP 369, 13560-970, São Carlos, SP, Brazil
[c] São Paulo State University (UNESP), Institute of Chemistry, 14800-060, Araraquara, SP, Brazil

ARTICLE INFO

Keywords:
Biosensors
RNA
Amplification-free
Viruses
Diagnosis

ABSTRACT

Viruses are infectious agents that cause various diseases worldwide. The recent COVID-19 pandemic has shown the need for rapid and reliable tests to confirm viral infections, aiming at the rapid isolation, treatment, and identification of high-incidence regions. Rapid antigen tests based on lateral flow immunochromatography have proven to be very useful. However, they are not accurate in patients with low viral loadings. The gold standard test is RT-PCR, which identifies parts of the viral genome by detecting specific DNA or RNA sequences. RT-PCR or similar tests such as RT-LAMP involve several steps for sample preparation and amplification of target sequences, require trained personnel to be performed, and can be time-consuming and expensive, limiting their point-of-care application. Biosensors are promising analytical devices for detecting nucleic acids, mainly RNA from viruses, offering advantages such as rapid results, high sensitivity, and low cost compared with the RT-PCR test since the amplification of target sequences is not necessary. Recently, several biosensors have been developed to detect RNA viruses without sequence amplification. Here, we present a review on the design and technology of amplification-free biosensors for the detection of viral RNA as an alternative for diagnosing infectious diseases. The challenges and advances for the point-of-care electrochemical, electrical, and optical biosensors will be addressed.

1. Introduction

Viruses are acellular microorganisms and intracellular parasites composed of two components: nucleic acid (single or double-stranded DNA or RNA) and a protein coat, known as the capsid, which is responsible for protecting the genome from host nucleases. They are considered devoid of their metabolic machinery since for propagation to occur, they depend on host cells that replicate the genetic material (Gelderblom, 1996). Several diseases are caused by viruses, including Ebola, MERS (Middle East Respiratory Syndrome), Influenza, Dengue, Zika, HIV/AIDS (Human Immunodeficiency Virus), and, most recently, the SARS-CoV-2 (Severe Acute Respiratory Syndrome Coronavirus 2), the pathologic agent of COVID-19 (coronavirus disease 2019) (Brazaca et al., 2021a).

COVID-19 has proven to be a significant public health problem, causing millions of deaths worldwide and a massive impact on the global economy. Other viral diseases such as Influenza, HIV, Zika, and Dengue can coexist in pandemic scenarios. In Brazil, from 2019 to 2022, during the COVID-19 pandemic, approximately 2.9 million cases of Dengue, 22.343 cases of Zika, and, 347.575 cases of Chikungunya were registered (Brasil. Ministério da Saúde. Secretaria de Vigilância em Saúde, n. d.). Differentiating viral diseases that present similar symptoms is crucial and the identification of nucleic acids (NAs) is the most effective way to confirm viral infections (Cantera et al., 2019).

The impact caused by the COVID-19 pandemic drew attention to the development and need for low-cost diagnosis of viral diseases, as well as the importance of society being prepared for future outbreaks. Additionally, since viruses exhibit high mutability, high resistance, and transmissibility, rapid diagnosis is essential for controlling the spread of viral diseases. Currently, the diagnostic method considered the gold standard for viral diseases is RT-PCR (Real-Time - Polymerase Chain Reaction) which demonstrates high sensitivity and specificity. However, it is an expensive and time-consuming test due to its steps, such as extraction, purification, conversion to DNA (in the case of RNA virus), and amplification of genetic material (Fig. 1). Moreover, this method requires qualified professionals, expensive reagents, and specialized

* Corresponding author.
E-mail address: ncsvieira@unifesp.br (N.C.S. Vieira).

https://doi.org/10.1016/j.biosx.2024.100478
Received 19 December 2023; Received in revised form 25 March 2024; Accepted 31 March 2024
Available online 12 April 2024

facilities (laboratory infrastructure), which implicates low accessibility and long response time for presenting results (Fraga et al., 2008).

Beyond RT-PCR, other tests follow similar steps for diagnosing viral diseases, such as RT-LAMP (Real-Time - Loop-Mediated Isothermal Amplification) and RPA (Recombinase Polymerase Amplification). RT-PCR, RT-LAMP, and RPA are very similar tests; the main difference is that in the LAMP and RPA tests, the genetic material is amplified at a predefined constant temperature, not requiring the use of a thermal cycler, which is robust and expensive (Lobato and O'Sullivan, 2018; Thompson and Lei, 2020). Additionally, RPA is a highly sensitive and selective isothermal amplification technique, operating at 37–42 °C, promising faster results than LAMP (Tan et al., 2022). Notably, the two techniques have high sensitivity and specificity but high operational costs.

Enhancing accessibility to diagnostics using the techniques mentioned above, especially in resource-limited regions, is a big challenge. There are research initiatives, exemplified by Bashir's group, which developed a rapid isothermal RT-LAMP amplification and portable detection system for SARS-CoV-2 (Ganguli et al., 2020). Their device could successfully detect ten clinical samples (five positives and five negatives) in 30 min without needing an RNA extraction kit (Ganguli et al., 2020). Also, notable commercial products have demonstrated the feasibility of bringing molecular diagnostics out of traditional laboratory settings and into decentralized environments (Carter et al., 2020). These include assay techniques and tests such as Visby (Katzman et al., 2023), Abbott ID NOW COVID-19 test (Babic et al., 2023), and the SARS-CoV-2 LAMP diagnostic assay (Color Genomics). These initiatives are significant despite facing challenges, such as specialized instruments, scalability, regulatory approval, and accuracy; they contribute to improved public health outcomes.

In addition to genetic tests, there are diagnostic methods based on the detection of viral antigens or antibodies produced in response to the virus infection (IgM and IgG), such as ELISA (Enzyme-Linked Immuno Sorbent Assay) and the lateral flow immunoassay, which were very explored for the COVID-19 diagnosis (Boonham et al., 2014a). Antigen tests indicate ongoing infection from the second or third day of symptoms. Conversely, antibody tests are recommended after the tenth day to detect active infection. These tests can also be used to assess prior infection or the effect of vaccination. The ELISA test is sensitive and specific. However, in addition to a long response time (hours or even days), it also requires laboratory structure and trained personnel, increasing its costs (Boonham et al., 2014b). The rapid tests may present cross-reactivity with other substances in the sample and depend on a high viral (or antibody) load to provide reliable results, which difficult the screening of asymptomatic people (Hsiao et al., 2021).

An alternative diagnosis for COVID-19 and other infections in high demand can be achieved with the use of biosensors as they offer advantages that meet most of the ASSURED criteria (Affordable, Sensitive, Specific, User-friendly, Rapid and Robust, Equipment-free, and Deliverable) established by the WHO (Naseri et al., 2022). These analytical devices can quickly provide information about disease biomarkers, including DNA and RNA sequences, and have the advantage of relatively simple construction (Brazaca et al., 2021b). In short, as shown in Fig. 2, these devices are comprised of three key elements: a biological recognition element that specifically recognizes the analyte; coupled to a physical-chemical detector known as the transducer; and the device to process the signal (Brazaca et al., 2021b). Biosensors for detecting nucleic acids (NAs) are called "genosensors". The classical recognition system is a single-stranded DNA (ssDNA) sequence capable of specifically hybridizing to an RNA or DNA target sequence (Brazaca et al., 2021b). Recently, CRISPR (clustered regularly interspaced short palindromic repeats) and CRISPR/Cas (associated proteins) technology has been used as a recognition system in biosensors to recognize NAs due to their remarkable genome editing ability (Li et al., 2019). CRISPR/Cas is a powerful, effective, and programmable tool that enables genetic cuts at designated target sites. This system has two fundamental parts: 1) the repetitive sequences, which are short DNA segments repeated multiple times in the bacterial genome, and 2) the spacer sequences, which are

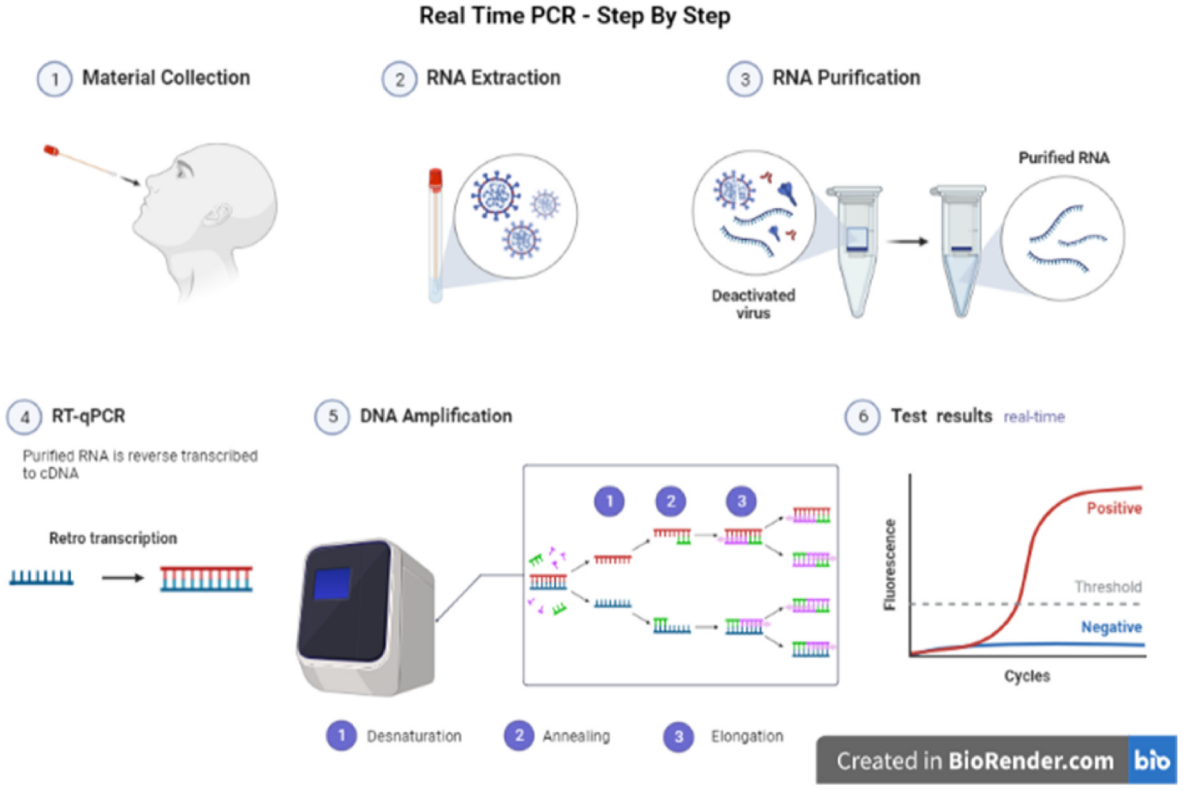

Fig. 1. Step by step of the RT-PCR analysis.

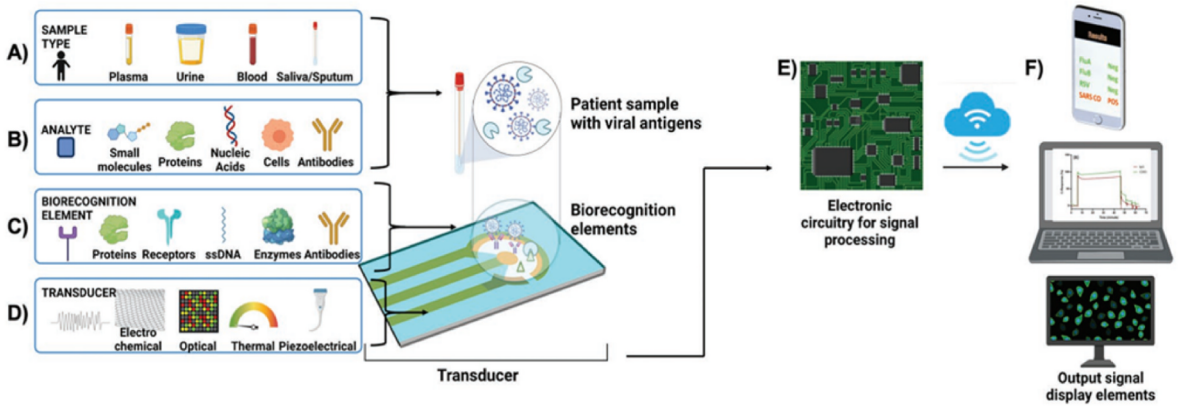

Fig. 2. Schematic representation of a biosensor including all elements: A) Sample types, including biofluids, such as plasma, urine, blood, or saliva/sputum for the analysis. B) Analytes that may be targeted for diagnoses, such as small molecules, proteins, nucleic acids, cells, and antibodies. C) Surface modification with bio-recognition elements such as proteins, receptors, ssDNA, enzymes, and antibodies. D) Signal conversion of biochemical interactions to electronic readout with a transducer. E) Electronic circuitry for signal processing, analysis, and transmission. F) Display of results. All images within this figure are adapted with permission from Biorender.com with a paid academic subscription (Kabay et al., 2022). Reprinted with permission from reference (Kabay et al., 2022). Copyright (2022) John Wiley & Sons.

DNA fragments derived from viruses or mobile genetic elements located among the repetitive sequences. Cas proteins capture and process the invaded DNA and use the spacer sequences to identify and delete similar DNA in the future. This system can be integrated with biosensors to enhance the traditional RNA/DNA diagnostic, taking advantage of its trans-cleavage activity (Chen et al., 2023).

An important limitation for point-of-care purposes relies on the amplification of the NA sequence. Since they are at a low concentration in typical samples, it is necessary to increase the sequence copies to reach a detectable concentration. This review presents the recent advances in the amplification-free detection of viral RNA using biosensors. The strategies and analytical techniques employed are discussed in detail. Challenges and perspectives for the improvement of biosensor performance aiming at a user-friendly and sensitive method are also presented. The following sections are dedicated to the types of biosensors according to the transduction method. Section 2 addresses the electrochemical biosensors; section 3 presents the electrical biosensors; and section 4 the optical biosensors. Section 5 highlights the challenges and perspectives regarding biosensors for the non-amplified detection of viral RNA sequences.

We direct the reader's attention toward the comparisons among various technologies, as their limit of detection (LODs) or operational ranges are presented in disparate units, considering the specific context and goals of the study analyzed. Furthermore, particular biosensors were employed to detect synthetic NA sequences in buffer solutions or in a medium (such as saliva). In contrast, others were used to discriminate between positive and negative clinical specimens.

It is important to compare the LOD of a new biosensor with the gold standard RT-PCR test. However, in RT-PCR, LOD can vary due to factors such as assay design and the targeted virus, often reported as viral RNA copies per reaction or milliliter of sample. RT-PCR for nasopharyngeal samples typically exhibits a LOD of ca. 100 copies/mL of transport media for COVID-19 diagnosis (Arnaout et al., 2021). The unit pfu/mL denotes infectious viral particles uncommon in RT-PCR assays. Mass/-volume units like mg/mL are suitable when quantifying in a pure solution of synthetic NA. Similarly, mol/L expresses substance concentration in moles per liter, potentially applicable if the NA sample is highly purified and uniform. Converting between these units requires additional specific information about the NA sequences analyzed, which is often unavailable in most analytical settings. While LODs are quantitative, results for virus identification testing are typically reported qualitatively as positive or negative.

2. Electrochemical biosensors

Electrochemical genosensors are designed for the analysis of RNA or DNA molecules. The hybridization event between the target RNA and the complementary ssDNA probe immobilized on the sensor surface leads to changes in the electrochemical properties of the system (Brazaca et al., 2021b). Traditional electrochemical techniques, such as amperometry, cyclic voltammetry (CV), differential pulse voltammetry (DPV), and electrochemical impedance spectroscopy (EIS), are used to analyze the hybridization event. Electrochemical genosensors offer several advantages for RNA analysis, including high sensitivity, selectivity, and specificity (Brazaca et al., 2021b). The main application of these devices is in diagnosis, mainly for virus-caused diseases, because they can detect RNA molecules with high precision, even in complex biological samples (Liu et al., 2023). Below we reviewed the electrochemical genosensors for the amplification-free detection of viral RNA. Table 1 summarizes the electrochemical genosensor with their LOD, disease, and analytical technique.

A study carried out by Wu et al. presented an amplification-free genosensor using the EIS for the detection of synthesized RNA fragments and Dengue virus amplicons (Wu et al., 2020a). This genosensor demonstrated good hybridization efficiency and selectivity for the Dengue serotype 1 (DENV1), with a LOD of 20 PFU/mL and a linear range of 10^2–10^5 PFU/mL. The signal for DENV1 was significantly higher than for the other serotypes (DENV2, DENV3, and DENV4), achieving a good selectivity (93.5 %–97.6 %). This study showed that the RNA probe density control method significantly influences the construction of RNA genosensors, especially with the use of binary self-assembled monolayer (SAM) (Wu et al., 2020b).

In the first few months of 2020, one of the biggest challenges in diagnosing COVID-19 was the limited availability of accurate and efficient diagnostic tests. Several research groups with expertise in biosensors started studies for the detection of COVID-19. In this context, Del Caño et al. presented a genosensor for the amplification-free and label-free detection of SARS-CoV-2 in patient samples using gold nanotriangles functionalized with oligonucleotides, as shown in Fig. 3 (Del Caño et al., 2022a). The gold nanotriangles deposited on screen-printed carbon electrodes provide a selective surface for the –SH group, which covalently reacts with gold, resulting in the proper spacing of the capture probes. The genosensor demonstrated a LOD of 22.2 fM, featured with DPV, and could detect point mutations in the virus genome (Del Caño et al., 2022b). Assays performed on swab samples from nasopharyngeal tests of patients with COVID-19 showed the ability to distinguish

Table 1
Some electrochemical genosensors with their limit of detection and analytical technique.

Reference	Strategy	Target	Limit of detection (LOD)	Electrochemical method
Wu et al. (2020a)	Binary SAM	Dengue virus	20 PFU/mL	EIS
Del Caño et al. (2022a)	Gold nanotriangles functionalized with oligonucleotides	SARS-CoV-2	22.2 fM	Differential Pulse Voltammetry (DPV)
Zambry et al. (2023b)	Printed circuit board gold substrate (PCBGE) with N protein as a biomarker	SARS-CoV-2	0.50 μM	CV and EIS
Heo et al. (2022a)	Cas13a trans-cleavage activity	SARS-CoV-2	4.4×10^{-2} fg/mL for the ORF gene and 8.1×10^{-2} fg/mL for the S gene	CV and EIS
Kashefi-Kheyrabadi et al. (2022b)	genosensor based on four-way junction (4-WJ) hybridization	SARS-CoV-2	5.0 and 6.8 ag/μL, (10^{-18} g/μL) for the S and Orf1ab genes, respectively.	CV and EIS
Kashefi-Kheyrabadi et al. (2023a)	CRISPR	SARS-CoV-2	2.5 for the S gene and 4.5 ag/μL for the Orf1ab gene	Square Wave Voltammetry (SWV)
Pina-Coronado et al. (2022a)	Methylene-blue functionalized carbon dots (CDs) combined with different shape gold nanostructures	SARS-CoV-2	2.0 aM	CV and DPV
Sheta et al. (2020a)	metal-organic nickel structure (Ni-MOF) with polyaniline nanocomposite	HCV	0.75 fM	EIS
El-Sheikh et al. (2021b)	Bimetallic organic platform containing silver and zinc	HCV	0.064 fM	DPV

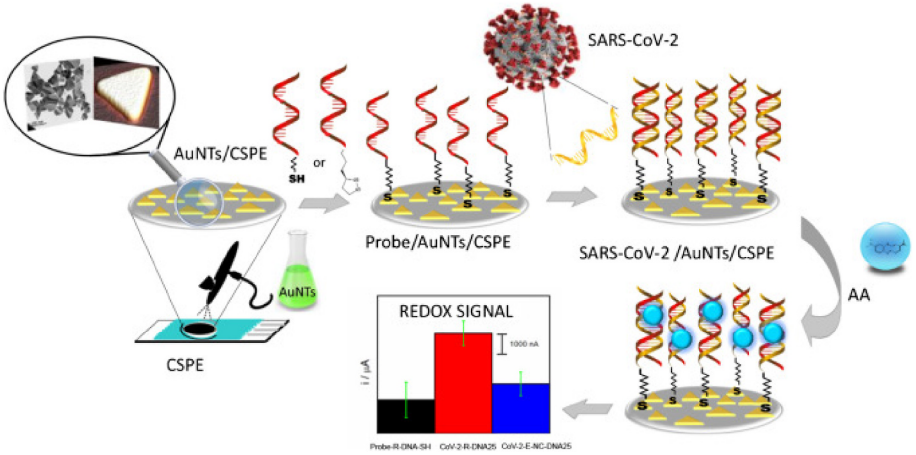

Fig. 3. Design of the biosensor development Reprinted with permission from reference (Del Caño et al., 2022b). Copyright (2022) Springer Nature.

between infected and uninfected patients, in addition to identifying patients with different viral loads, without any amplification method. The results were well correlated to the analyses performed by RT-PCR in the same samples (Del Caño et al., 2022b).

Zambry et al. developed a label-free genosensor for detecting SARS-CoV-2 on a printed circuit board with a gold substrate (PCBGE) (Zambry et al., 2023a). The biosensor used the nucleocapsid phosphoprotein (N) gene as a biomarker and detected up to 1 copy/μL of the N gene in 5 min, with a LOD of 0.5 μM, using CV and EIS. Biosensor performance was evaluated with synthetic SARS-CoV-2 RNA and 20 clinical RNA samples with minimal sample preparation (Zambry et al., 2023b). The negative clinical samples showed a mean value of charge transfer resistance (R_{ct}) of 2.17 kΩ, while in the positive samples the mean R_{ct} was 4.91 kΩ, a remarkable difference for discrimination. The proposed biosensor is a promising device for POC analysis due to its fast detection time and the possibility of integration with a microfluidic system. However, further investigations are still needed on the surface modification of the PCBGE-conjugated gold electrode and microfluidic platforms (Zambry et al., 2023b).

The possibility of identifying polymorphisms in the hybridization event allows genosensors to investigate specific genes of viral agents. Some studies have explored this possibility, such as the study developed by Heo et al. in which a genosensor amplification-free was used to detect the ORF and S genes of SARS-CoV-2 through Cas13a trans-cleavage activity (Heo et al., 2022a). The biosensor was able to detect concentrations ranging from 1.0×10^{-1} to 1.0×10^{5} fg/mL, with LOD estimated at 4.4×10^{-2} fg/mL for the ORF gene and 8.1×10^{-2} fg/mL for the S gene. This biosensor showed good reproducibility, with variations intra- and inter-assay from 2.47% to 3.14% for the ORF gene and from 1.74% to 2.52% for the S gene (Heo et al., 2022b). The quantification of 1.0×10^{7} fg/mL was achieved for the first time in saliva samples from patients using the proposed detection platform. (Heo et al., 2022b). The sensing accuracy was validated using artificial saliva spiked with SARS-CoV-2 RNA sequences. The results demonstrate that the biosensor is viable for detecting SARS-CoV-2 RNA with high precision in saliva samples, making large-scale diagnosis feasible and providing the necessary speed for times of pandemic. A schematic illustration of the sensing strategy proposed by Heo et al. is presented in Fig. 4 (Heo et al., 2022b).

In another investigation with the same target genes, Kashefi-Kheyrabadi et al. developed a genosensor based on four-way junction (4-WJ) hybridization for amplification-free detection of SARS-CoV-2 RNA (Kashefi-Kheyrabadi et al., 2022a). The results of the analysis of 21 clinical samples, using the techniques of CV and EIS, were concordant with the results of the same analyses with RT-PCR showing the ability to distinguish between positive and negative samples. The biosensor was considered stable for two weeks, and the intra- and inter-day reproducibility was less than or equal to 10% for the S and Orf1ab genes. The LOD for these viral genes was 5.0 and 6.8 ag/μL, (10^{-18} g/μL) respectively, with an assay time of 1 h. The LOD thresholds are beneath the viral burden found in clinical specimens, providing the biosensor with the requisite sensitivity to identify SARS-CoV-2 during the initial phases

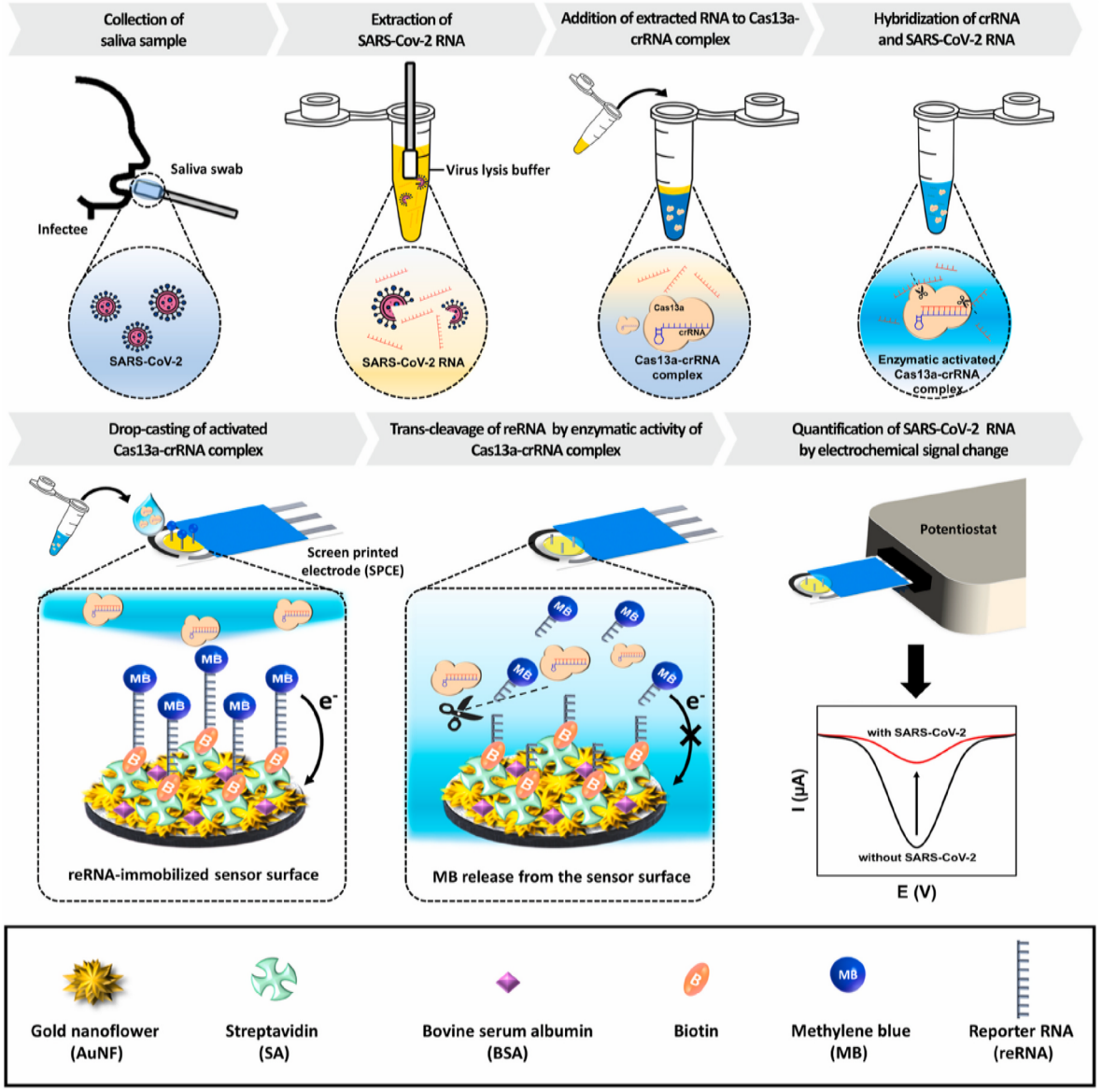

Fig. 4. Schematic illustration of the proposed electrochemical biosensing strategy utilized with the CRISPR/Cas13a for SARS-CoV-2 detection. Viral RNA is extracted from saliva collected from infected patients using the lysis buffer and mixed with a Cas13a–crRNA complex-containing solution. This complex binds with the SARS-CoV-2 RNA, resulting in enzymatic activity. The activated Cas13a–crRNA complex is subsequently loaded onto the sensor surface for cleaving the reRNA immobilized on the electrode. The presence of SARS-CoV-2 can be quantified via analysis of the current change. Reprinted with permission from reference (Heo et al., 2022b). Copyright (2022) Elsevier.

of the illness when the viral genetic load is minimal (Kashefi-Kheyrabadi et al., 2022b).

Kashefi-Kheyrabadi et al. refined the previously reported genosensor for COVID-19 by incorporating CRISPR to cleave the sequence to be identified, Fig. 5 shows the schematic of the detection platform (Kashefi-Kheyrabadi et al., 2023a). The amplification-free genosensor was used to analyze SARS-CoV-2 RNA fragments in synthetic and clinical samples. The LOD was 2.5 for the S gene and 4.5 ag/μL for the Orf1ab gene, providing specificity and simplicity to the proposed platform. Synthetic RNA with different nucleotide sequences, including Influenza-A, was used as a specificity test. Control experiments confirmed that the CRISPR platform can only detect SARS-CoV-2 RNA sequences when all components are present. The final concentration of each sequence in the solution was 5×10^{13} M. The results are promising since the biosensor achieved excellent specificity in differentiating target sequences from related RNA sequences and low LOD (Kashefi--Kheyrabadi et al., 2023b).

Many strategies have been used to improve the selectivity and sensitivity of electrochemical biosensors for PCR amplification-free detection. The use of nanomaterials, in particular, can be advantageous due to their high surface area and bio affinity that could increase the electrochemical signal and, consequently, the sensitivity. Carbon-based nanomaterials such as nanotubes, nanosheets, and quantum dots have shown significant interest due to the abundance of surface functional groups, simple synthesis protocols, and tunable electrochemical active surfaces (Wang and Dai, 2015).

Carbon dots (CDs) are known to have a stronger interaction with double-strand (dsDNA) than with ssDNA. Recently, functionalized carbon dots with methylene blue (MB-CDs), which is a redox indicator, were combined with a mixture of spherical and triangular gold nanoparticles (AuNps) for SARS-CoV-2 RNA detection (Fig. 6) (Pina-Coronado et al., 2022a). The gold nanostructures increase the electrode surface area and the number of active sites, improving the biosensing layer development. The MB-CDs are electrochemically active and can

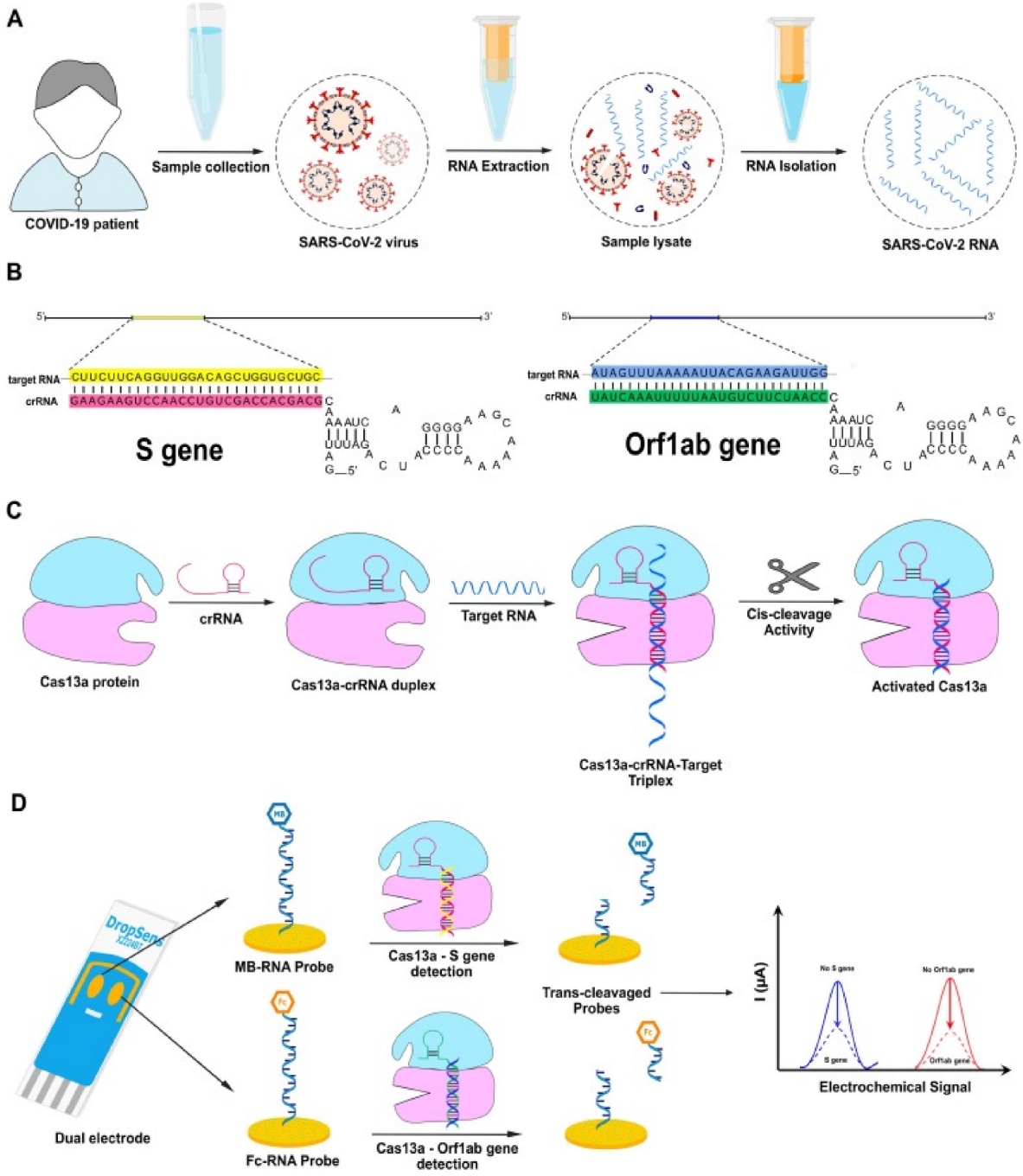

Fig. 5. Schematic of the detection platform (A) The extraction of SARS-CoV-2 RNA sequences from COVID-19 patients' samples. (B) The S and Orf1ab single-stranded target RNA (highlighted in yellow and blue, respectively) as well as the S and Orf1ab crRNA (highlighted in pink and green, respectively). (C) A conformational change in Cas13a in response to crRNA and target RNA binding results in non-target collateral cleavage. (D) The E-CRISPR working principle and its main components. The redox probe conjugated reRNA-modified biosensor is exposed to the enzymatically activated Cas13a-crRNA-target RNA triplex. Activated Cas 13a cleaves the reRNA, resulting in the release of the redox probe from the reRNA and eventually, a decrease in the electrochemical signal. Reprinted with permission from reference (Kashefi-Kheyrabadi et al., 2023b). Copyright (2023) Elsevier. (For interpretation of the references to color in this figure legend, the reader is referred to the Web version of this article.)

interact efficiently with dsDNA, indicating the hybridization event (Pina-Coronado et al., 2022a). The device was characterized by CV, scanning electron microscopy (SEM), and atomic force microscopy (AFM) (Pina-Coronado et al., 2022a). DPV measurements were used to achieve higher sensitivity and improve the discrimination between signal and background current (Pina-Coronado et al., 2022a). This device presented a LOD of 2 aM in DNA samples. In addition, the biosensor showed a higher response (1.2 ± 0.2 μA) in case of infection compared to the non-infected cases (0.80 ± 0.08 μA) for RNA nasopharyngeal samples without any amplification process (Pina-Coronado et al., 2022b).

In the study conducted by Sheta et al., an unlabeled probe was developed for the direct detection of unamplified hepatitis C virus RNA (HCV-RNA) (Sheta et al., 2020a). The platform was built using a metal-organic nickel structure (Ni-MOF) with polyaniline nanocomposite and showed sensitivity and specificity in EIS assays in the range of 1 fM to 100 nM, even in the presence of non-specific NAs. This biosensor also showed high stability, maintaining 90.76 % of its initial

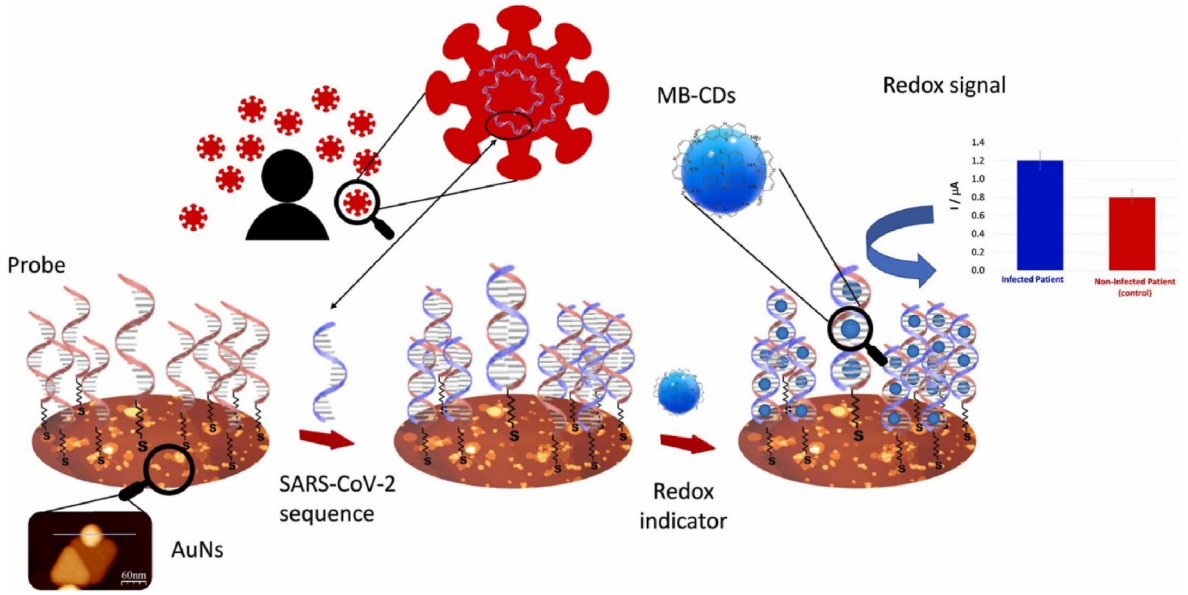

Fig. 6. Design of the biosensor. Functionalized carbon dots with methylene blue (MB-Cds), a redox indicator, are integrated with a spherical and triangular AuNps blend to detect SARS-CoV-2 RNA. Reprinted with permission from reference [20]. Copyright (2022) Elsevier. (For interpretation of the references to color in this figure legend, the reader is referred to the Web version of this article.)

response to a 1 pM target after 28 days of storage at 4 °C with a LOD of 0.75 fM. Assay reproducibility was confirmed by intra- and inter-assay relative standard deviations, which were 3.65 % and 3.27 %, respectively. The promising results from this study include the development of a label-free electrochemical genosensor with high sensitivity, specificity, and long-term stability for the quantitative determination of unamplified HCV (Sheta et al., 2020b).

El-Sheikh et al. presented an evolution of the previous proposal to develop an electrochemical RNA biosensor for detecting HCV in patient samples. This genosensor was structured on a bimetallic organic platform containing silver and zinc (Ag/Zn-MOF) for the direct detection of amplification-free NA. The biosensor exhibited a linear response for the concentration range from 1 fM to 100 nM and a LOD of 0.64 fM in DPV assays. In specificity tests, the biosensor demonstrated a significant increase in current with complementary RNA (10 pM) compared to non-complementary RNA (100 pM) (El-Sheikh et al., 2021a). The biosensor also showed good stability, without significant changes during the first three days of storage at 4 °C, preserving 91.34 % of its initial response after 35 days of storage. Biosensor reproducibility was high, with relative standard deviations of 3.34 % and 2.97 % for intra-assay and inter-assay, respectively. The reliability of the biosensor was tested using spiking experiments with different concentrations of HCV targets (1 pM, 10 pM, and 100 nM) in diluted human serum samples. The design has the potential to compete with current commercial HCV monitoring assays and offers a mechanism to develop new biosensors for other pathogens (El-Sheikh et al., 2021b).

3. Electrical biosensors

In this section, two types of electrical biosensors are addressed for the non-amplified detection of RNA sequences: electrical biosensors based on non-faradaic impedance spectroscopy (EI) and field-effect transistors devices. Despite different operating principles, the capacitance formed due to the electrical double layer of an electrode immersed in an electrolyte plays a fundamental role in both devices (Luo and Davis, 2013). In EI-based biosensors, an AC potential (alternating current) of low amplitude with variable frequencies is applied between two electrodes separated by a distance d. The system can be modeled as a parallel plate capacitor, and events that occur between or on the electrodes change the capacitance of the system (Zucolotto et al., 2007). Elements such as interfacial capacitance, charge transfer resistance, solution resistance, and Warburg coefficient (ZW), among others, contribute to these changes (Afsarimanesh et al., 2020).

Although there are several EI-based biosensors available for the detection of different disease biomarkers, there have been limited studies for detecting non-amplified RNA. Cheng et al. used interdigitated electrodes for the non-amplified detection of Zika virus RNA sequences (Cheng et al., 2017a). The authors used interdigitated aluminum electrodes modified with specific capture probes to detect a particular region of the Zika virus genome. The sensor successfully detected unamplified Zika virus RNA sequences in just 30 s and with high specificity. The genosensor demonstrated a wide operating range of 187–1,876,000 copies/µL and a LOD of 158.1 copies/mL (Cheng et al., 2017b).

The other electrical biosensors discussed here are those based on FET transducers (Fernandes et al., 2010, 2022a). Bergveld et al. introduced in the 1970s the ISFET (ion-sensitive field-effect transistor) device for measuring ions in a physiological medium. The ISFET is similar to a conventional MOSFET (metal-oxide-semiconductor field-effect transistor). The essential difference is that a metal/electrolyte interface replaces the metal/oxide gate interface. In the MOSFET, the channel current (I_{DS}, source-drain current) is controlled by the gate voltage (V_{GS} - gate-source voltage) in a purely capacitive process since the gate oxide is insulating. In an ISFET, the channel current is also controlled by the gate voltage (Fernandes et al., 2022b). However, ionic conduction from the electrolyte leads to the formation of electric double layers (EDLs) at the metal/electrolyte and electrolyte/gate oxide interfaces (Fernandes et al., 2022b).

Exposing the channel directly to the electrolyte (without the presence of the gate oxide) offers advantages for biosensing purposes, particularly when nanostructured semiconductor materials form the channel. FETs usually have an improved signal due to the highest surface-to-volume ratio of nanomaterials. This allows the detection of analytes, including RNA sequences, at very low concentrations. An ssDNA sequence or a CRISP/Cas system explicitly targeting RNA is immobilized onto the FET channel. When hybridization or a cleavage occurs, a change in charge shifts the current between the source and drain electrodes of the FET (Fernandes et al., 2022b). FETs composed of graphene or its derivatives are outstanding in detecting non-amplified

NAs because graphene is extremely sensitive to electric fields in its vicinity (Fernandes et al., 2022b).

Hajian et al. reported a graphene FET associated with a CRISPR/Cas system for the label-free detection of unamplified target genes (Hajian et al., 2019a). Graphene was modified with a catalytically deactivated Cas9 CRISPR complex, which interacts with its target sequence by scanning the whole genomic sample and unzipping the double helix when necessary. The authors demonstrated the detection of several NA sequences related to several diseases. Specifically, for viruses, sequences related to lentiviruses were detected (Hajian et al., 2019b).

Li et al. immobilized single-strand phosphorodiamidate morpholino oligos (PMO) sequences, an uncharged DNA analog, on reduced graphene oxide FETs modified with AuNPs for amplification-free detection of SARS-CoV-2 RNA (Li et al., 2021a). Throat swab samples from patients are extracted and immersed in a virus-preserving solution, followed by treatment with a solution to lyse the cell. After centrifugation, the final suspension was applied directly onto the rGO FET (named G-FET nanosensor) (Li et al., 2021b). Fig. 7 shows the schematic diagram of the trial proposed by the authors. The total test time was 32 min, 30 min for sample preparation, and 2 min for biosensor analysis. Tests with the biosensors showed an excellent response with PCR tests on samples from 20 patients with COVID-19 and 10 healthy individuals (Li et al., 2021b).

Recently, Li et al. improved the previous rGO FET using a CRISPR/Cas13a system (Li et al., 2022a). Cas13 acts as a CRISPR RNA (crRNA)-guided RNA-targeting ribonuclease (Li et al., 2022b). This new system was used for the unamplified detection of coronavirus (CoV) and hepatitis C virus (HCV). Under optimized conditions, the sensor provided a low LOD of 1.5×10^4 (25 aM) and 2.65×10^4 copies/mL (44 aM) for the CoV ORF1ab CoV N genes, respectively. Clinical applicability was also confirmed by distinguishing HCV-infected from normal controls (Li et al., 2022b).

Yu et al. used the same CRISPR/Cas13a recognition system for the unamplified detection of SARS-CoV-2 RNA (Yu et al., 2022a). The difference from Li's study is that the gold gate electrode (Au) was functionalized with the CRISPR/Cas13a system instead of the FET channel (see Fig. 8). Also, the device used a CVD (chemical vapor deposition) graphene instead of rGO to achieve a solution-gated graphene FET (SGGTs) (Yu et al., 2022b). Ten clinical samples from 5 COVID-19 patients and five healthy individuals could be distinguished and had LOD 1.3×10^{-17} M and 4.0×10^{-16} M for synthetic gene fragments and serum/throat swab samples, respectively (Yu et al., 2022b).

A graphene FET biosensor modified with a triple-probe tetrahedral DNA framework (TDF) dimer as a capture probe was developed by Wu et al. for SARS-CoV-2 RNA detection (Wu et al., 2022a). The three probes were designed specifically for SARS-CoV-2 RNA at the ORF1ab, RdRp, and E genes (Wu et al., 2022b). These probes showed a synergic effect, improving the binding affinity and enabling the biosensor to directly detect 0.025–0.05 copies/μL SARS-CoV-2 RNA in artificial saliva. Without a requirement for NA amplification, the biosensor distinguished positive cases from negative ones using nasopharyngeal swab samples from patients. It can be used as 10 - in - 1 pooled testing, proving the potential in screening COVID-19 and other epidemic diseases [9]. Fig. 9 illustrates the workflow of the test using the termed triple-probe TDF dimer g-FET (graphene-FET) proposed by Wu et al. (2022b). Table 2 summarizes the electrical genosensors with their LOD, disease, and analytical technique.

More recently, a portable carbon nanotube FET was shown by Liang et al. for the amplification-free detection of SARS-CoV-2 (Liang et al., 2023). Using a multi-probe strategy, the biosensor detected SARS-CoV-2 antigens or RNA without amplifying to a single virus level within 1 min In clinical tests, a combined detection strategy of the two systems allowed the distinction of 10 COVID-19 patients from 10 healthy individuals (Liang et al., 2023).

4. Optical biosensors

We present here some optical biosensors used to diagnose viral diseases in the RNA amplification-free strategy. The measurements obtained with optical biosensors are extremely sensitive, highly selective, and fast to detect biomolecules, such as NAs, featured in this review. Optical biosensors are classified based on the transducer used, which can be colorimetry, fluorescence, optofluidic devices, fiber optics, and surface plasmon resonance (SPR), which is the most used (Singh et al., 2023).

Several optical biosensors for virus detection have focused on nanoparticle applications to improve sensitivity and selectivity. In particular, the optical properties of gold nanoparticles (AuNPs) are widely explored due to the SPR phenomenon, which provides to these nanomaterials intense color and high extinction coefficient, an essential advantage over conventional dyes (Shawky et al., 2017a). These optical properties are related to their size, shape, concentration, and colloidal stabilization, which depend on the synthesis method and stabilization agents. Generally, the AuNPs suspension is red or pink and changes to purple-blue upon aggregation. The color of the sample associated with its colloidal stabilization is the working principle of colorimetric detection (Moitra et al., 2020). In optical biosensors, aggregation of AuNPs results from the binding of the analyte to their surface, which can

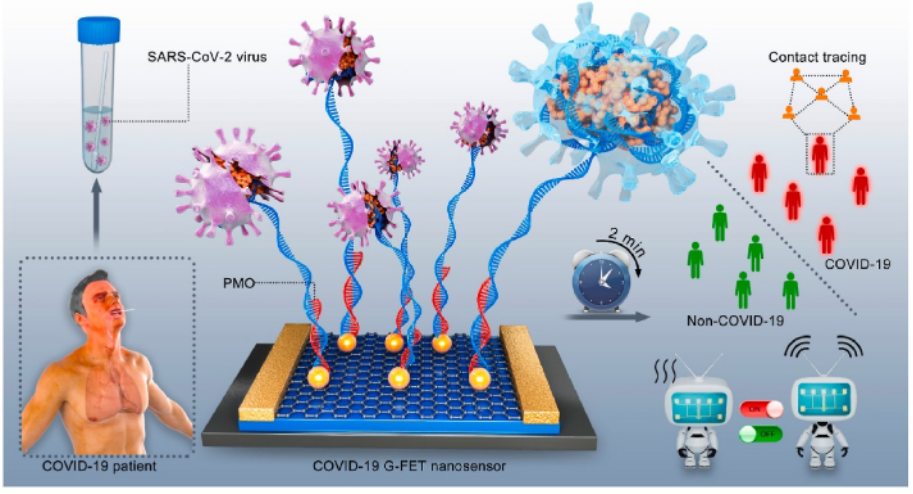

Fig. 7. Schematic diagram of PCR-free rapid direct identification of COVID-19 using the PMO-functionalized G-FET nanosensor. Reprinted with permission from reference (Li et al., 2021b). Copyright (2021) Elsevier.

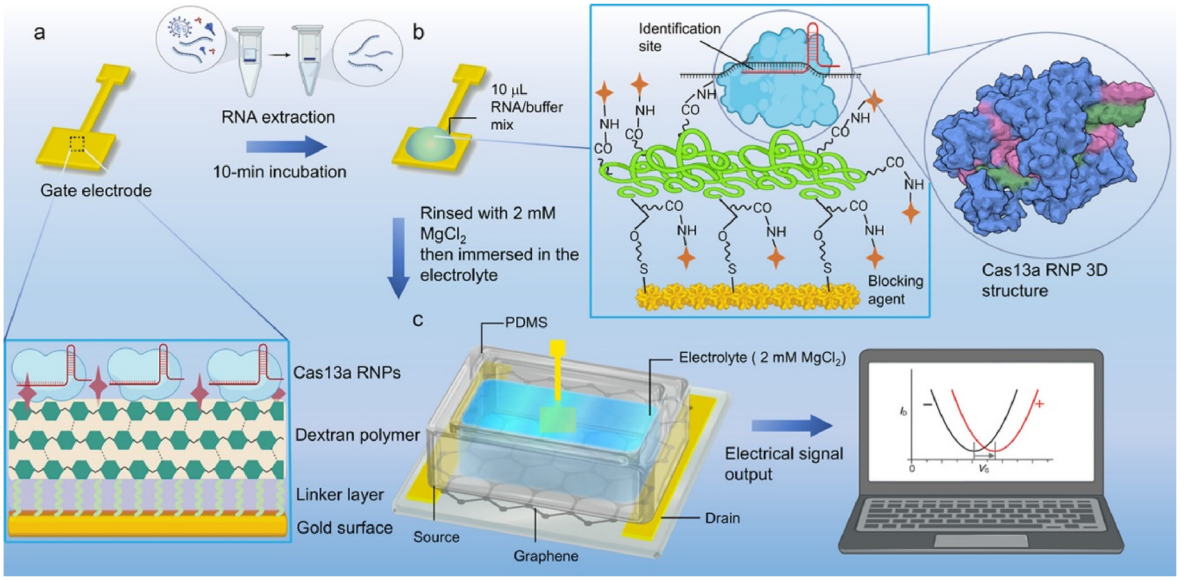

Fig. 8. Design and sensing principle of CRISPR/Cas13a-modified SGGTs. (a) Schematic diagram of the sensing layer structure. (b) Schematic diagram of the sensing principle (PDB, 5XWP). (c) The characterization process of converting biological signals into electrical signals. Created with BioRender.com. Reprinted with permission from reference (Yu et al., 2022b). Copyright (2021) Elsevier.

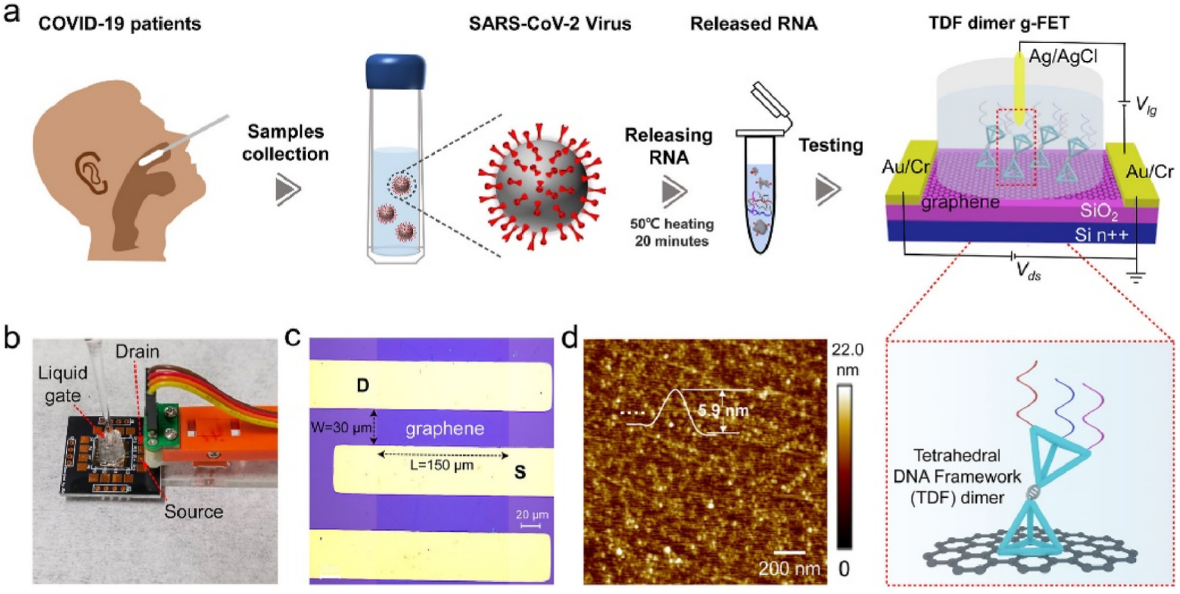

Fig. 9. Triple-probe TDF dimer g-FET sensor for SARS-CoV-2 RNA testing. (a) Workflow and schematic diagram of the triple-probe TDF dimer g-FET sensor for SARS-CoV-2 RNA testing. The enlarged diagram is the g-FET sensing surface modified with a triple-probe TDF dimer. (b) Digital photograph of a working device. (c) Optical microscope image of the g-FET channel. (d) AFM image of the sensing surface after triple-probe TDF dimer immobilization (measured in fluid). Reprinted with permission from reference (Wu et al., 2022b). Copyright (2022) American Chemical Society.

be measured by collecting the absorption spectrum, where a broadening and displacement of the SPR band is observed, or with the naked eye observation of the color change (Borghei et al., 2022a; Moitra et al., 2020; Molaabasi et al., 2022a; Shawky et al., 2017a).

Borghei et al. proposed an optical biosensor without RNA extraction and amplification based on colorimetry (visual monitoring) to detect SARS-CoV-2 (Borghei et al., 2022a). To reduce these two steps in the detection procedure, AuNPs were capped with an antisense oligonucleotide (ASO) ssDNA synthesized to be complementary to a target RNA sequence. Four sets of ASOs were prepared with an extra strand polyguanine (G12) tail at the 5′end of ASO1 and ASO3 and the 3′end of ASO2 and ASO4 to work as a template for in situ formation of AuNPs (Fig. 10). The positive and negative SARS-CoV-2 samples were collected and divided into two groups: one received the full treatment (RNA extraction and amplification), and the other was used directly (without pre-processing). Transmission electron microscopy (TEM) images and UV–Vis spectra were collected from both groups. In the positive sample, the color was changed from red to purple and the SPR band shifted from 530 nm to 575 nm, indicating the aggregation of the AuNPs. By using four ASOs@AuNPs, this biosensor demonstrated high specificity and selectivity, offering a simple and fast (5 min) test for the point-of-care diagnosis of viral pathogens just by changing the ASO format (Borghei et al., 2022b). Furthermore, this biosensor can be based on direct detection microfluidic paper-based analytical device (μPAD), which offers rapid detection, cost-effectiveness, ease of use, portability, minimal sample volume requirement (a mixture of 5 μL of probes

Table 2
Some electrical genosensors with their limit of detection and analytical technique.

Reference	Strategy	Target	Limit of detection (LOD)	Electrical method
Hajian et al. (2019a)	CRISPR/Cas technology to label-free detect unamplified target genes along a graphene FET	Lentiviruses	1.7 fM	Graphene FET
Li et al. (2021a)	Phosphorodiamidate morpholino oligos (PMO) sequences, on reduced graphene oxide FET modified with gold nanoparticles	SARS-CoV-2	0.37 fM	Graphene oxide FET
Li et al. (2022a)	CRISPR/Cas13a with reduced graphene oxide FET modified with gold nanoparticles	SARS-CoV-2 and Hepatitis C	25 aM	Graphene oxide FET
Yu et al. (2022a)	CRISPR/Cas13a	SARS-CoV-2	1.3×10^{-17} M	Graphene FET
Wu et al. (2022a)	Graphene FET modified with a triple-probe tetrahedral DNA framework dimer	SARS-CoV-2	158.1 copiess/uL	Graphene FET

(ASOs@AuNPs), and 3 μL of samples containing SARS-CoV-2 virus), and a LOD comparable to RT-PCR (Borghei et al., 2022b). For the same purpose, Parikshit Moitra et al. developed an optical biosensor that applied ASOs@AuNPs and colorimetric measurements to diagnose COVID-19 without performing the RNA extraction process [33]. The AuNPs were coated with thiol-modified ASOs specific for N-gene of SARS-CoV-2. In this optical biosensor, the aggregation of the thiolated ASOs@AuNPs only occurred in the presence of the target RNA sequence of SARS-CoV-2 resulting in a shift of the SPR band. The aggregation of ASOs@AuNPs in the presence of SARS-CoV-2 RNA (with a LOD of 10 copies/μL) was measured by UV–Vis spectra, transmission electron microscopy (TEM), and enhanced dark-field hyperspectral imaging technique (Moitra et al., 2020). A preclinical screening and high sensitivity with minimal false positives could be obtained by this colorimetric biosensor with adaption to target other regions of the viral genomic material, such as S-gene (surface glycoprotein), E-gene (envelope protein), and M-gene (membrane glycoprotein) (Moitra et al., 2020).

Shawky et al. conducted a study using AuNPs in a colorimetric biosensor for the direct quantification of hepatitis C virus RNA in clinical samples (Shawky et al., 2017b). The goal was to induce the aggregation employing positively charged AuNPs (cysteamine and CTAB-capped AuNPs) in citrate-capped AuNPs that were functionalized with a thiolated HCV RNA-specific probe (nanoprobe) (Shawky et al., 2017b). The HCV-specific nanoprobes were incubated with HCV viral RNA (positive sample) or non-specific RNA (negative sample). For the negative samples, the color of the suspension changed from red to blue, which indicates that the cysteamine AuNPs electrostatically bound to the phosphate backbone of the nanoprobes inducing their aggregation. In the positive samples, the red color of the suspension was maintained since the hybridized target RNA keeps the cationic AuNPs away from the nanoprobes. This biosensor presented 93.3 % sensitivity, high specificity, and LOD of 4.57 IU/uL (Shawky et al., 2017b).

Du et al. developed a fluorescence-based biosensor for the

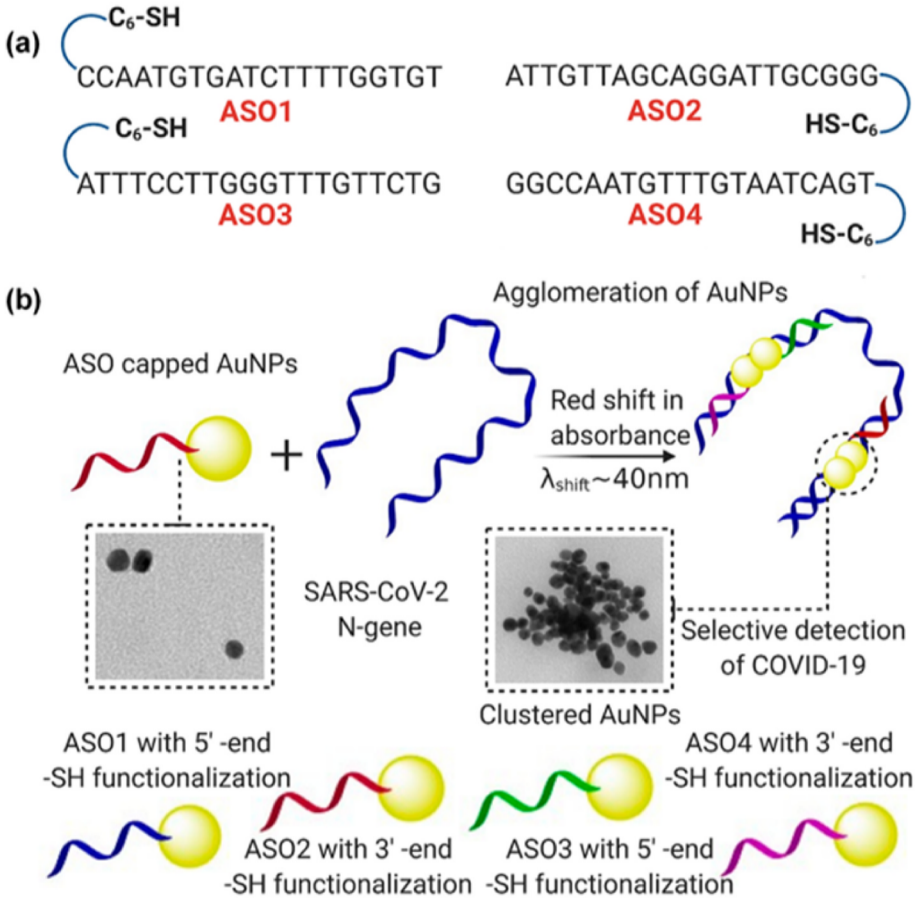

Fig. 10. Differentially functionalized ASOs with their sequences are represented in (a). The proposed concept behind the agglomeration of gold nanoparticles, when capped with the ASOs, is schematically presented in (b). Reprinted with permission from reference (Moitra et al., 2020). Copyright (2020) Elsevier.

amplification-free detection of the Ebola virus in a point-of-care form on a multiplexed on-chip for sample preparation (Du et al., 2017). This optofluidic platform, *i.e.*, an antiresonant reflecting optical waveguide (ARROW) chip has provided some microfluidic features such as small sample volume, flexibility, and affordability, which become important advantages for developing a biosensor. However, in the micrometer-scale channels and reservoirs, the mixing of regents is a challenge. To overcome this limitation, a system of metered air bubble injection and thermally stable beads was incorporated in the chip to be a simple and efficient proceeding without including complex chip modifications. Compared with the previous version, which used in-valve target capture and streptavidin beads, this new version of the chip enhanced capture efficiency by 2 orders in magnitude, keeping the limit equal to 0.21 pfu/mL (Du et al., 2017). A laser at 433 nm wavelength, approximately 70 mW average power, was focused on the sample with a diameter of 1 mm, and the fluorescence emission signal was collected using a fiber spectrometer. The signal peak at 537 nm indicated a linear dependence with NA concentration. Therefore, this result determined the sample capture efficiency. For the extraction process, the nucleic acid targets are pumped and mixed with a suspension of magnetic microbeads conjugated with a capture probe on the incubation reservoirs. After enhancing capture by stirring up the beads, the air bubbles are pumped through the reservoirs (Du et al., 2017). By hybridizing with capture probes, the targets with matched sequences are captured. To separate between the beads and the mismatched sequence, a magnet is used to pull down the beads while the mismatched sequence becomes supernatant. At high temperatures, the beads are washed to remove weakly bound nonspecific sequences. Captured targets are released from the magnetic beads by denaturing the double-strand hybrid with heat. Finally, the released targets are stained by SYBR® Gold dye and detected using the ARROW chip. With similar sensitivity as PCR, this biosensor propounded elevated sensitivity, specificity, and a wide dynamic range required for a practical clinical assay, despite the complexity found in the microchip setup (Du et al., 2017).

Molaabasi et al. developed a fluorescence-based biosensor to detect the SARS-CoV-2 virus without RNA further amplification, fluorophore, or design with a special DNA fragment (Molaabasi et al., 2022b). This device is based on cytosine-modified ASOs specific for either N gene or RdRP genes that can form silver nanoclusters (AgNCs) in the presence of the SARS-CoV-2 target RNA sequence, thereby emerging dual-emission ratiometric signal transduction (green and red emission) (Molaabasi et al., 2022b). In this setup, the introduction of GO as a platform to enhance aggregation-induced emission was tested to improve the sensitivity and specificity of the sensor. The fluorescence intensity signal reveals that a competition mechanism may exist between aggregation-induced emission and aggregation-caused quenching (ACQ) influenced by the whole probe structure with GO added (Molaabasi et al., 2022b). Results from 150 clinical samples indicated elevated sensitivity and selectivity (>90 %) for detection with low cost, reliable, reproducible, in 12 min, and offering a LOD of 0.30–10.0 nM. In addition to these advantages, this biosensor proposes a switching DNA sensor that could behold with easy to use, one-step synthesis, small volume sample (5 μL), thiol-free, robust equipment-free, linker-free conjugation, genome amplification-free, working at room temperature, and no need of modification, labeling, and even centrifuging to remove excess ions from the reaction solution (Molaabasi et al., 2022b). Besides, this device can be adapted to target other viral genome regions. It can be applied in different techniques used in biosensors for preclinical screening with minimal false results (Molaabasi et al., 2022b).

In 2021, Sampad et al. reported the amplification-free detection of SARS-CoV-2 RNAs using an optofluidic nanopore sensor and optical trapping technology (Sampad et al., 2021). The optofluidic nanopore sensor relies on a silicon substrate containing a pore with 20 nm of diameter integrated into a microfluidic channel for controlled sample delivery (Sampad et al., 2021). Magnetic beads conjugated with complementary sequences were employed to capture the target RNA and separated from the clinical nasopharyngeal swab samples using a magnet. A single optical beam was applied to trap the beads at the nanopore, and the optofluidic sensor was heated to induce the release of the target sequences from the beads. The translocation of individual RNA targets through the nanopore causes remarkable changes in the ionic current. This sensor detected SARS-CoV-2 RNAs in the clinically relevant concentration range, with a LOD of 17 aM, showing promise for COVID-19 diagnosis (Sampad et al., 2021).

Addressing the need for a highly sensitive method to detect NA sequences without prior amplification, Yang et al. developed an endonuclease-dependent molecular beacon probe (DEMBA) for the detection of ssDNA and ssRNA sequences through fluorescence measurements or lateral flow assay (Yang et al., 2019). The molecular beacons (MBe) comprise four functional regions that form two hairpins, as shown in Fig. 11 (Yang et al., 2019). In the native MBe structure, the 3′ and 5′ ends are very close; however, when hybridizing with the target sequence, its structure changes, generating an endonuclease recognition site. Then, MBe is cleaved by endonuclease, and three fragments are obtained. The 3′ and 5′ ends of the native framework are on different fragments (Yang et al., 2019). To obtain a fluorescence signal in response to target recognition, the MBe was labeled with a fluorophore at the 5′ end and a quencher at the 3′ end. In the native MBe, the fluorescence signal is very low, since the fluorophore and quencher are close. After hybridization with the target sequence and endonuclease digestion, the labels separate, and the fluorescence signal increases. Also, the target sequence is available to bind to another MBe, so the signal is amplified. This method achieved excellent sensitivity, as ssDNA and ssRNA sequences below 1 pM and 10 pM, respectively, were detected (Yang et al., 2019).

For colorimetric detection using a lateral flow dipstick, MBe was labeled with biotin at the 5′ end and fluorescein at the 3′ end. The dipstick conjugation zone was modified with colorimetric probes coated with anti-biotin antibodies. Antibodies against fluorescein (anti-fluorescein) form the test line, and the control line contains secondary antibodies against anti-biotin (anti-anti-biotin) (Yang et al., 2019). For the native MBe, the biotin interacts with the anti-biotin onto the colorimetric probes. The complex formed is captured in the test line by binding fluorescein with their antibodies. The remaining colorimetric probes bind to the control line (Yang et al., 2019). For a sample without the target sequence, both lines are colored. When the sample contains the target sequence, the endonuclease will cleave the MBe. Since biotin and fluorescein will be in different fragments, the fragment containing fluorescein will be captured in the test line. However, it will not be labeled with the colorimetric probes. Consequently, only the control line will be colored. Using this strategy, a LOD of 10 pM was obtained for both ssDNA and ssRNA sequences (Yang et al., 2019).

Heidari et al. reported two colorimetric biosensors to detect the RNA from the Bovine viral diarrhea virus (BVDV), which causes several diseases characterized by acute diarrhea and lesions in the gastrointestinal tract in ruminants (Heidari et al., 2021). RNA detection was performed using two strategies: the cross-linking (CL) and non-crosslinking (NCL) of AuNPs functionalized with DNA probes. In the CL-based test, AuNPs are conjugated to two DNA probes complementary to different parts of the target. Hybridization between the probes and the target causes the formation of a network where the nanoparticles are closer together, resulting in visible aggregates (Heidari et al., 2021). Therefore, the color of the suspension changes from red to blue when there is a target sequence but remains red in its absence. For NCL-based testing, AuNPs are functionalized with a single type of DNA probe. When adding salt in high concentration, the cations neutralize the negative charge of the AuNPs, causing their aggregation and a change in the color of the suspension. However, hybridization with the target sequence prevents salt-induced aggregation, and the red color of the suspension is maintained (Heidari et al., 2021). The study showed that both methods could detect RNA without amplification, but the LC-based test is more sensitive. Although this strategy is promising, its sensitivity (6.83

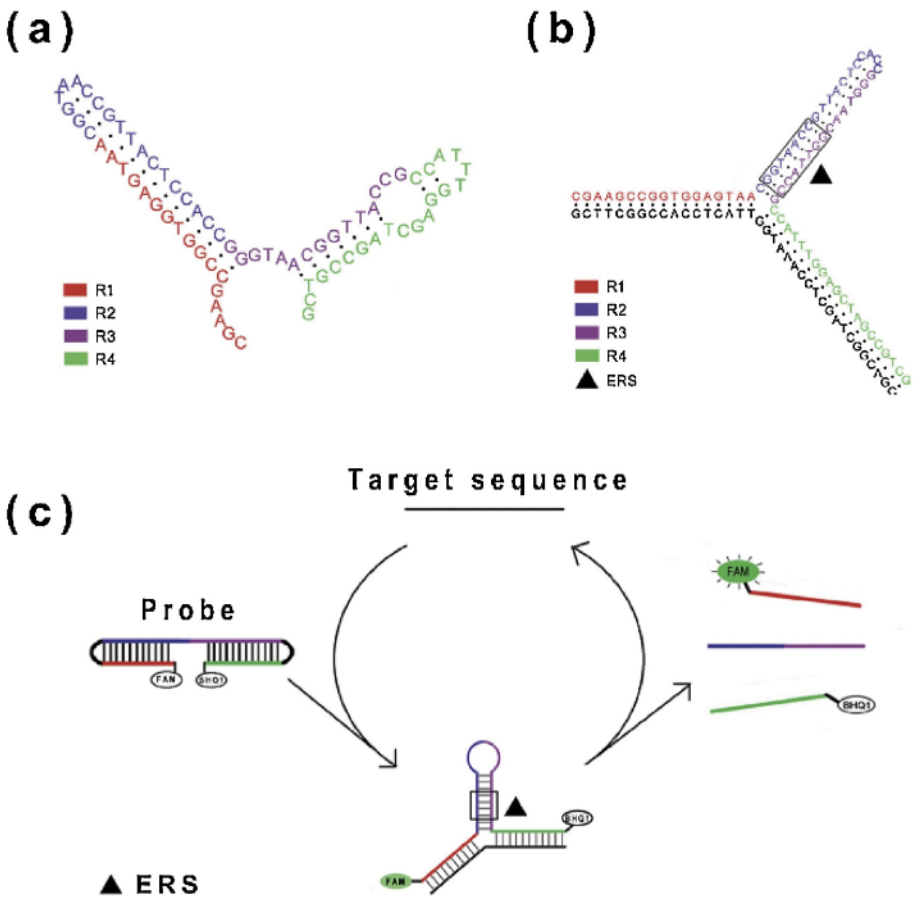

Fig. 11. General principle of DEMBA. R1-4: region 1–4; ERS: endonuclease recognition site. (a) The inactive structure of DEMBA probe. (b) The active structure of DEMBA probe. (c) The cyclical reaction process of basic DEMBA. Reprinted with permission from reference [31]. Copyright (2021) Elsevier.

ng/reaction) was much lower than that obtained by multiplex nested RT-PCR (4×10^{-4} ng/reaction) and real-time RT-PCR (12.4×10^{-2} ng/reaction), showing that improvements are still needed (Heidari et al., 2021).

An ultrasensitive DNA amplification-free biosensor was developed by Pang et al. for the detection of an RNA sequence indicated as high pathogenicity influenza (HPAI) virus biomarker (Pang et al., 2014). A metal film over the nanosphere (MFON) was functionalized with DNA strands tagged to a Raman label molecule to obtain a SERS-active substrate. These sequences have a hairpin structure that keeps the Raman

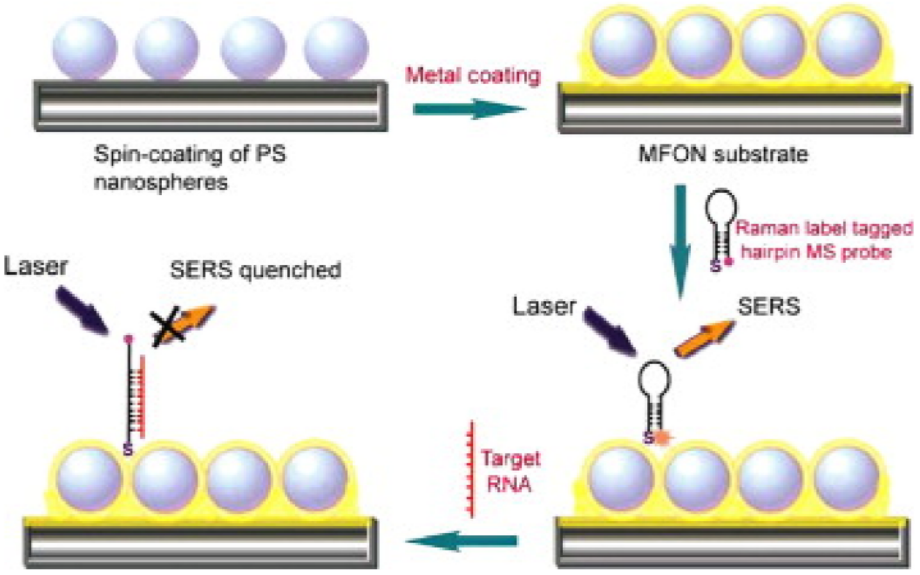

Fig. 12. Scheme of the manufacture and detection principle for the RNA marker. Reprinted with permission from reference (Pang et al., 2014). Copyright (2014) Elsevier.

label close to the surface, resulting in intense Raman scattering. However, when the probes hybridize with the target sequence, the hairpin structure is opened, and the Raman label is pulled away from the substrate, decreasing the scattering (Fig. 12) (Pang et al., 2014). A linear relationship between the diminished Raman signal and the target RNA concentration was obtained for 0–60 amol. The biosensor presented a LOD of 2.67 amol, corresponding to the RNA extracted from 60000 cells. This indicates that it can detect real samples without DNA amplification (Pang et al., 2014).

Aiming at a nucleic acid detection system without pre-amplification, Yin et al. developed a Surface-enhanced Raman scattering (SERS)-based biosensor integrating a chimeric DNA/RNA hairpin and CRISPR/Cas12a to generate a very sensitive optical response to the presence of the target sequence (Yin et al., 2022). In the first step, the endonuclease enzyme (Cas12a)/crRNA complex is activated by binding to the target sequence. The activated complex cleaves the chimeric RNA/DNA hairpin, used as a displacer, releasing the RNA. AuNps of 13 nm tagged to ultrabright Raman reporter are bounded to 40 nm-AuNps. The binding between them occurs due to the partial hybridization between ssDNA1 onto the surface of 13 nm-AuNPs and ssDNA2, which covers the 40-nm AuNPs. The RNA released by the activated Cas12a/crRNA complex fully complements ssDNA2. As this binding is energetically more favorable, ssDNA1 is replaced by RNA, and the 13 nm-AuNps labeled with Raman probes are dissociated from the 40 nm-AuNPs (Yin et al., 2022). Therefore, the target sequence triggers this cascade resulting in a significant decrease in the Raman signal. As a proof of concept, the system was tested to detect the Orf gene of SARS-CoV-2, and a LOD of 10 aM (~6000 copies/mL) was obtained. In addition, they showed that when using magnetic nanoparticles to separate AuNPs, the sensitivity was increased, resulting in a LOD of 1 aM (~600 copies/mL) (Yin et al., 2022).

In summary, Table 3 presents the optical biosensors with their LOD, target disease, and analytical technique.

5. Final remarks and perspectives

The recent COVID-19 pandemic showed that technological advances in diagnosing viral diseases, especially in devices with high applicability, low cost, and rapid diagnosis, are crucial for managing pandemic situations. This review highlights that biosensors are highly cost-effective devices, demonstrating comparable reliability to gold standard tests such as RT-PCR, RT-LAMP, and ELISA, in addition to demand less infrastructure and trained personnel to carry out the tests efficiently. The detection of amplification-free RNA is very advantageous since the amplification step, employed to increase the RNA concentration, is time-consuming, expensive, and requires robust equipment, which makes point-of-care analysis difficult. All the studies discussed here refer to biosensing systems in which detection is sensitive enough to not require the amplification step. The distinction between positive and negative cases of viral infections has confirmed the clinical applicability of biosensors. Some diseases selectively detected were SARS-CoV-2, Dengue, Hepatitis C, Lentivirus, Ebola, and Influenza. Different analytical techniques were explored. The most common methods for electrochemical biosensors are amperometry, cyclic voltammetry (CV), differential pulse voltammetry (DPV), and electrochemical impedance spectroscopy (EIS). Electrical biosensors include non-faradaic impedance spectroscopy (EI) and field-effect transistors. Regarding optical biosensors, colorimetry, fluorescence, and surface plasmon resonance (SPR) were the most explored.

Many studies combined biosensors with CRISPR/Cas technology to increase sensitivity and specificity. Although biosensors associated with the CRISPR/Cas system offer advantages, there are still some limitations regarding designing the system for efficient and accurate detection without unspecific sequences being recognized and cleaved and maintaining the stability of the components during the process. Furthermore, implementing this system in genosensors may require specialized

Table 3
Some optical biosensors with their limit of detection and analytical technique.

Reference	Strategy	Target	Limit of detection (LOD)	Optical method
Shawky et al. (2017a)	The aggregation induction using positively charged AuNPs (cysteamine and CTAB-capped AuNPs) in citrate-capped AuNPs functionalized with a thiolated HCV RNA-specific probe (nanoprobe)	Hepatitis C	4.57 IU/uL	Colorimetric
Moitra et al. (2020)	The aggregation of the thiolated ASOs@AuNPs only occurred in the presence of the target RNA sequence of SARS-CoV-2 resulting in a shift of the SPR band, without performing the RNA extraction process.	SARS-CoV-2	10 copies/μL	Colorimetric
Molaabasi et al. (2022b)	The cytosine-modified ASOs specific for either N gene or RdRP genes that can form silver nanoclusters (AgNCs) in the presence of the SARS-CoV-2 target RNA sequence, thereby emerging dual-emission ratiometric signal transduction without amplification, fluorophore, or design with a special DNA fragment.	SARS-CoV-2	0.30–10.0 nM.	Fluorescence
Borghei et al. (2022a)	AuNPs were capped with ASO ssDNA synthesized to be complementary to a target RNA sequence without RNA extraction and amplification. The color was changed from red to purple, indicating the aggregation of the AuNPs.	SARS-CoV-2	10 copies/μL	Colorimetric
Du et al. (2017)	The amplification-free in a point-of-care multiplexed ARROW chip with mixing and thermally system using air bubbles.	Ebola virus	0.21 pfu/mL	Fluorescence and optofluidic

(continued on next page)

Table 3 (*continued*)

Reference	Strategy	Target	Limit of detection (LOD)	Optical method
Sampad et al. (2021)	The amplification-free optofluidic nanopore sensor relies on a silicon substrate containing a pore with 20 nm of diameter integrated into a microfluidic channel for controlled sample delivery	SARS-CoV-2	17 aM	Optofluidic nanopore sensor and optical trapping technology
Yang et al. (2019)	Development of an endonuclease-dependent molecular beacon probe (DEMBA) without amplification.	ssDNA and ssRNA sequences	1 pM for ssDNA and 10 pM for ssRNA.	Fluorescence measurements or lateral flow assay
Heidari et al. (2021)	Two strategies: the cross-linking (CL) and non-crosslinking (NCL) of AuNPs functionalized with DNA probes.	Bovine viral diarrhea virus	6.83 ng/reaction	Two colorimetric
Pang et al. (2014)	A metal film over the nanosphere (MFON) was functionalized with DNA strands tagged to a Raman label molecule to obtain a SERS-active substrate. These sequences have a hairpin structure that keeps the Raman label close to the surface, resulting in intense Raman scattering without amplification.	influenza (HPAI) virus	2.67 amol	Surface-enhanced Raman scattering (SERS)
Yin et al. (2022)	Development of a chimeric DNA/RNA hairpin and CRISPR/Cas12a to generate a very sensitive optical response without pre-amplification.	Orf gene of SARS-CoV-2	1 aM (~600 copies/mL)	Surface-enhanced Raman scattering (SERS)

equipment, reagents, and expertise, adding to the overall cost and complexity.

We can conclude that biosensors are promising technologies for amplification-free viral RNA detection. However, efforts must be made for the concept reviewed here to leave the research laboratory and reach the market, benefiting the population. Such efforts include: (i) carrying out more tests with biosensors to achieve relevant statistics, (ii) miniaturization of measurement systems aiming at a final product, (iii) tests with other types of viral diseases, (iv) partnerships between universities and research centers with companies.

CRediT authorship contribution statement

Brenda G. Parassol: Writing – review & editing, Writing – original draft, Methodology, Formal analysis, Conceptualization. **Nayla Naomi Kusimoto Takeuti:** Writing – review & editing, Writing – original draft, Validation, Methodology, Conceptualization. **Henrique Antonio Mendonça Faria:** Writing – review & editing, Writing – original draft, Visualization, Validation, Methodology, Formal analysis, Conceptualization. **Kelly C. Jorge:** Writing – review & editing, Writing – original draft, Visualization, Validation, Methodology, Investigation, Formal analysis, Conceptualization. **Isabella Sampaio:** Writing – review & editing, Writing – original draft, Visualization, Validation, Methodology, Investigation, Formal analysis, Conceptualization. **Valtencir Zucolotto:** Writing – review & editing, Writing – original draft, Visualization, Validation, Supervision, Project administration, Methodology, Investigation, Funding acquisition, Formal analysis, Conceptualization. **Nirton C.S. Vieira:** Writing – review & editing, Writing – original draft, Visualization, Validation, Supervision, Project administration, Methodology, Investigation, Formal analysis, Conceptualization.

Declaration of competing interest

There is no conflict of interest.

Data availability

No data was used for the research described in the article.

Acknowledgements

The authors are grateful for the financial support provided by the National Council for Scientific and Technological Development, CNPq (309943/2020-5 and 408339/2023-3).

References

Afsarimanesh, N., Nag, A., Alahi, M.E.E., Han, T., Mukhopadhyay, S.C., 2020. Interdigital sensors: biomedical, environmental and industrial applications. Sens. Actuators A Phys. 305, 111923.

Arnaout, R., Lee, R.A., Lee, G.R., Callahan, C., Cheng, A., Yen, C.F., Smith, K.P., Arora, R., Kirby, J.E., 2021. The limit of detection matters: the case for benchmarking severe acute respiratory syndrome coronavirus 2 testing. Clin. Infect. Dis. 73, e3042–e3046.

Babic, N., Garner, K.S., Hirschhorn, J.W., Zebian, R., Nolte, F.S., 2023. Evaluation of Abbott ID NOW COVID-19 POC test performance characteristics and integration in the regional health network workflows to improve health care delivery. Clin. Biochem. 117, 69–73.

Boonham, N., Kreuze, J., Winter, S., van der Vlugt, R., Bergervoet, J., Tomlinson, J., Mumford, R., 2014a. Methods in virus diagnostics: from ELISA to next generation sequencing. Virus Res. 186, 20–31.

Boonham, N., Kreuze, J., Winter, S., van der Vlugt, R., Bergervoet, J., Tomlinson, J., Mumford, R., 2014b. Methods in virus diagnostics: from ELISA to next generation sequencing. Virus Res. 186, 20–31.

Borghei, Y.-S., Samadikhah, H.R., Hosseinkhani, S., 2022a. Exploitation of N-gene of SARS-CoV-2 to develop a new rapid assay by ASOs@ AuNPs. Anal. Chem. 94, 13616–13622.

Borghei, Y.-S., Samadikhah, H.R., Hosseinkhani, S., 2022b. Exploitation of N-gene of SARS-CoV-2 to develop a new rapid assay by ASOs@ AuNPs. Anal. Chem. 94, 13616–13622.

Brasil. Ministério da Saúde. Secretaria de Vigilância em Saúde, n.d. Boletins Epidemiológicos [WWW Document]. URL https://www.gov.br/saude/pt-br/centrais-de-conteudo/publicacoes/boletins/epidemiologicos/edicoes (accessed 6. February.2023)..

Brazaca, L.C., Dos Santos, P.L., de Oliveira, P.R., Rocha, D.P., Stefano, J.S., Kalinke, C., Muñoz, R.A.A., Bonacin, J.A., Janegitz, B.C., Carrilho, E., 2021a. Biosensing strategies for the electrochemical detection of viruses and viral diseases–A review. Anal. Chim. Acta 338384.

Brazaca, L.C., Dos Santos, P.L., de Oliveira, P.R., Rocha, D.P., Stefano, J.S., Kalinke, C., Muñoz, R.A.A., Bonacin, J.A., Janegitz, B.C., Carrilho, E., 2021b. Biosensing strategies for the electrochemical detection of viruses and viral diseases–A review. Anal. Chim. Acta 338384.

Cantera, J.L., White, H., Diaz, M.H., Beall, S.G., Winchell, J.M., Lillis, L., Kalnoky, M., Gallarda, J., Boyle, D.S., 2019. Assessment of eight nucleic acid amplification technologies for potential use to detect infectious agents in low-resource settings. PLoS One 14, e0215756.

Carter, L.J., Garner, L.V., Smoot, J.W., Li, Y., Zhou, Q., Saveson, C.J., Sasso, J.M., Gregg, A.C., Soares, D.J., Beskid, T.R., 2020. Assay Techniques and Test Development for COVID-19 Diagnosis.

Chen, D., Huang, W., Zhang, Y., Chen, B., Tan, J., Yuan, Q., Yang, Y., 2023. CRISPR-Mediated profiling of viral RNA at single-nucleotide resolution. Angew. Chem. 135, e202304298.

Cheng, C., Wu, J., Fikrig, E., Wang, P., Chen, J., Eda, S., Terry, P., 2017a. Unamplified RNA sensor for on-site screening of Zika virus disease in a limited resource setting. Chemelectrochem 4, 485–489.
Cheng, C., Wu, J., Fikrig, E., Wang, P., Chen, J., Eda, S., Terry, P., 2017b. Unamplified RNA sensor for on-site screening of Zika virus disease in a limited resource setting. Chemelectrochem 4, 485–489.
Color Genomics, SARS-CoV-2 LAMP diagnostic assay, May, 18, 2020.
Del Caño, R., García-Mendiola, T., García-Nieto, D., Álvaro, R., Luna, M., Iniesta, H.A., Coloma, R., Diaz, C.R., Milán-Rois, P., Castellanos, M., 2022a. Amplification-free detection of SARS-CoV-2 using gold nanotriangles functionalized with oligonucleotides. Microchim. Acta 189, 171.
Del Caño, R., García-Mendiola, T., García-Nieto, D., Álvaro, R., Luna, M., Iniesta, H.A., Coloma, R., Diaz, C.R., Milán-Rois, P., Castellanos, M., 2022b. Amplification-free detection of SARS-CoV-2 using gold nanotriangles functionalized with oligonucleotides. Microchim. Acta 189, 171.
Du, K., Cai, H., Park, M., Wall, T.A., Stott, M.A., Alfson, K.J., Griffiths, A., Carrion, R., Patterson, J.L., Hawkins, A.R., 2017. Multiplexed efficient on-chip sample preparation and sensitive amplification-free detection of Ebola virus. Biosens. Bioelectron. 91, 489–496.
El-Sheikh, S.M., Osman, D.I., Ali, O.I., Shousha, W.G., Shoeib, M.A., Shawky, S.M., Sheta, S.M., 2021a. A novel Ag/Zn bimetallic MOF as a superior sensitive biosensing platform for HCV-RNA electrochemical detection. Appl. Surf. Sci. 562, 150202.
El-Sheikh, S.M., Osman, D.I., Ali, O.I., Shousha, W.G., Shoeib, M.A., Shawky, S.M., Sheta, S.M., 2021b. A novel Ag/Zn bimetallic MOF as a superior sensitive biosensing platform for HCV-RNA electrochemical detection. Appl. Surf. Sci. 562, 150202.
Fernandes, E.G.R., Faria, H.A.M., Vieira, N.C.S., 2022a. Field-effect transistors for biomedical applications. In: Advances in Bioelectrochemistry, vol. 3. Springer, pp. 1–30.
Fernandes, E.G.R., Faria, H.A.M., Vieira, N.C.S., 2022b. Field-effect transistors for biomedical applications. In: Advances in Bioelectrochemistry, vol. 3. Springer, pp. 1–30.
Fernandes, E.G.R., Vieira, N.C.S., De Queiroz, A.A.A., Guimarães, F.E.G., Zucolotto, V., 2010. Immobilization of poly(propylene imine) dendrimer/nickel phtalocyanine as nanostructured multilayer films to be used as gate membranes for SEGFET pH Sensors. J. Phys. Chem. C 114, 6478–6483. https://doi.org/10.1021/jp9106052.
Fraga, D., Meulia, T., Fenster, S., 2008. Real-time PCR. Curr. Protoc. Essent. Lab. Tech 10–13.
Ganguli, A., Mostafa, A., Berger, J., Aydin, M.Y., Sun, F., Ramirez, S.A.S. de, Valera, E., Cunningham, B.T., King, W.P., Bashir, R., 2020. Rapid isothermal amplification and portable detection system for SARS-CoV-2. In: Proceedings of the National Academy of Sciences, vol. 117, pp. 22727–22735.
Gelderblom, H.R., 1996. Structure and Classification of Viruses, fourth ed. Medical Microbiology.
Hajian, R., Balderston, S., Tran, T., DeBoer, T., Etienne, J., Sandhu, M., Wauford, N.A., Chung, J.-Y., Nokes, J., Athaiya, M., 2019a. Detection of unamplified target genes via CRISPR–Cas9 immobilized on a graphene field-effect transistor. Nat. Biomed. Eng. 3, 427–437.
Hajian, R., Balderston, S., Tran, T., DeBoer, T., Etienne, J., Sandhu, M., Wauford, N.A., Chung, J.-Y., Nokes, J., Athaiya, M., 2019b. Detection of unamplified target genes via CRISPR–Cas9 immobilized on a graphene field-effect transistor. Nat. Biomed. Eng. 3, 427–437.
Heidari, Z., Rezatofighi, S.E., Rastegarzadeh, S., 2021. Development and comparison of cross-linking and non-crosslinking probe-gold nanoparticle hybridization assays for direct detection of unamplified bovine viral diarrhea virus-RNA. BMC Biotechnol. 21, 1–12.
Heo, W., Lee, K., Park, S., Hyun, K.-A., Jung, H.-I., 2022a. Electrochemical biosensor for nucleic acid amplification-free and sensitive detection of severe acute respiratory syndrome coronavirus 2 (SARS-CoV-2) RNA via CRISPR/Cas13a trans-cleavage reaction. Biosens. Bioelectron. 201, 113960.
Heo, W., Lee, K., Park, S., Hyun, K.-A., Jung, H.-I., 2022b. Electrochemical biosensor for nucleic acid amplification-free and sensitive detection of severe acute respiratory syndrome coronavirus 2 (SARS-CoV-2) RNA via CRISPR/Cas13a trans-cleavage reaction. Biosens. Bioelectron. 201, 113960.
Hsiao, W.W.-W., Le, T.-N., Pham, D.M., Ko, H.-H., Chang, H.-C., Lee, C.-C., Sharma, N., Lee, C.-K., Chiang, W.-H., 2021. Recent advances in novel lateral flow technologies for detection of COVID-19. Biosensors 11, 295.
Kabay, G., DeCastro, J., Altay, A., Smith, K., Lu, H., Capossela, A.M., Moarefian, M., Aran, K., Dincer, C., 2022. Emerging biosensing technologies for the diagnostics of viral infectious diseases. Adv. Mater. 34, 2201085.
Kashefi-Kheyrabadi, L., Nguyen, H.V., Go, A., Baek, C., Jang, N., Lee, J.M., Cho, N.-H., Min, J., Lee, M.-H., 2022a. Rapid, multiplexed, and nucleic acid amplification-free detection of SARS-CoV-2 RNA using an electrochemical biosensor. Biosens. Bioelectron. 195, 113649.
Kashefi-Kheyrabadi, L., Nguyen, H.V., Go, A., Baek, C., Jang, N., Lee, J.M., Cho, N.-H., Min, J., Lee, M.-H., 2022b. Rapid, multiplexed, and nucleic acid amplification-free detection of SARS-CoV-2 RNA using an electrochemical biosensor. Biosens. Bioelectron. 195, 113649.
Kashefi-Kheyrabadi, L., Nguyen, H.V., Go, A., Lee, M.-H., 2023a. Ultrasensitive and amplification-free detection of SARS-CoV-2 RNA using an electrochemical biosensor powered by CRISPR/Cas13a. Bioelectrochemistry, 108364.
Kashefi-Kheyrabadi, L., Nguyen, H.V., Go, A., Lee, M.-H., 2023b. Ultrasensitive and amplification-free detection of SARS-CoV-2 RNA using an electrochemical biosensor powered by CRISPR/Cas13a. Bioelectrochemistry, 108364.
Katzman, B.M., Wockenfus, A.M., Kelley, B.R., Karon, B.S., Donato, L.J., 2023. Evaluation of the Visby medical COVID-19 point of care nucleic acid amplification test. Clin. Biochem. 117, 1–3.
Li, Y., Li, S., Wang, J., Liu, G., 2019. CRISPR/Cas systems towards next-generation biosensing. Trends Biotechnol 37, 730–743.
Li, J., Tang, L., Li, T., Li, K., Zhang, Y., Ni, W., Xiao, M.-M., Zhao, Y., Zhang, Z.-Y., Zhang, G.-J., 2022a. Tandem cas13a/crRNA-mediated CRISPR-FET biosensor: a one-for-all check station for virus without amplification. ACS Sens. 7, 2680–2690.
Li, J., Tang, L., Li, T., Li, K., Zhang, Y., Ni, W., Xiao, M.-M., Zhao, Y., Zhang, Z.-Y., Zhang, G.-J., 2022b. Tandem Cas13a/crRNA-mediated CRISPR-FET biosensor: a one-for-all check station for virus without amplification. ACS Sens. 7, 2680–2690.
Li, J., Wu, D., Yu, Y., Li, T., Li, K., Xiao, M.-M.M., Li, Y., Zhang, Z.-Y.Y., Zhang, G.-J.J., 2021a. Rapid and unamplified identification of COVID-19 with morpholino-modified graphene field-effect transistor nanosensor. Biosens. Bioelectron. 183, 113206 https://doi.org/10.1016/j.bios.2021.113206.
Li, J., Wu, D., Yu, Y., Li, T., Li, K., Xiao, M.-M.M., Li, Y., Zhang, Z.-Y.Y., Zhang, G.-J.J., 2021b. Rapid and unamplified identification of COVID-19 with morpholino-modified graphene field-effect transistor nanosensor. Biosens. Bioelectron. 183, 113206 https://doi.org/10.1016/j.bios.2021.113206.
Liang, Y., Xiao, M., Xie, J., Li, J., Zhang, Yuyan, Liu, H., Zhang, Yang, He, J., Zhang, G., Wei, N., 2023. Amplification-free detection of SARS-CoV-2 down to single virus level by portable. Carbon Nanotube Biosensors. Small, 2208198.
Liu, L., Xu, Z., Molina Vargas, A.M., Dollery, S.J., Schrlau, M.G., Cormier, D., O'Connell, M.R., Tobin, G.J., Du, K., 2023. Aerosol jet printing-enabled dual-function electrochemical and colorimetric biosensor for SARS-CoV-2 detection. Anal. Chem. 95, 11997–12005.
Lobato, I.M., O'Sullivan, C.K., 2018. Recombinase polymerase amplification: basics, applications and recent advances. Trac. Trends Anal. Chem. 98, 19–35.
Luo, X., Davis, J.J., 2013. Electrical biosensors and the label free detection of protein disease biomarkers. Chem. Soc. Rev. 42, 5944–5962.
Moitra, P., Alafeef, M., Dighe, K., Frieman, M.B., Pan, D., 2020. Selective naked-eye detection of SARS-CoV-2 mediated by N gene targeted antisense oligonucleotide capped plasmonic nanoparticles. ACS Nano 14, 7617–7627.
Molaabasi, F., Kefayat, A., Ghasemzadeh, A., Amandadi, M., Shamsipur, M., Alipour, M., Moosavifard, S.E., Besharati, M., Hosseinkhani, S., Sarrami-Forooshani, R., 2022a. Role of the probe sequence/structure in developing an ultra-efficient label-free COVID-19 detection method based on competitive dual-emission ratiometric DNA-templated silver nanoclusters as single fluorescent probes. Anal. Chem. 94, 17757–17769.
Molaabasi, F., Kefayat, A., Ghasemzadeh, A., Amandadi, M., Shamsipur, M., Alipour, M., Moosavifard, S.E., Besharati, M., Hosseinkhani, S., Sarrami-Forooshani, R., 2022b. Role of the probe sequence/structure in developing an ultra-efficient label-free COVID-19 detection method based on competitive dual-emission ratiometric DNA-templated silver nanoclusters as single fluorescent probes. Anal. Chem. 94, 17757–17769.
Naseri, M., Ziora, Z.M., Simon, G.P., Batchelor, W., 2022. ASSURED-compliant Point-of-care Diagnostics for the Detection of Human Viral Infections.
Pang, Y., Wang, J., Xiao, R., Wang, S., 2014. SERS molecular sentinel for the RNA genetic marker of PB1-F2 protein in highly pathogenic avian influenza (HPAI) virus. Biosens. Bioelectron. 61, 460–465.
Pina-Coronado, C., Martínez-Sobrino, Á., Gutiérrez-Gálvez, L., Del Caño, R., Martínez-Periñán, E., García-Nieto, D., Rodríguez-Peña, M., Luna, M., Milán-Rois, P., Castellanos, M., 2022a. Methylene Blue functionalized carbon nanodots combined with different shape gold nanostructures for sensitive and selective SARS-CoV-2 sensing. Sensor. Actuator. B Chem. 369, 132217.
Pina-Coronado, C., Martínez-Sobrino, Á., Gutiérrez-Gálvez, L., Del Caño, R., Martínez-Periñán, E., García-Nieto, D., Rodríguez-Peña, M., Luna, M., Milán-Rois, P., Castellanos, M., 2022b. Methylene Blue functionalized carbon nanodots combined with different shape gold nanostructures for sensitive and selective SARS-CoV-2 sensing. Sensor. Actuator. B Chem. 369, 132217.
Sampad, M.J.N., Zhang, H., Yuzvinsky, T.D., Stott, M.A., Hawkins, A.R., Schmidt, H., 2021. Optical trapping assisted label-free and amplification-free detection of SARS-CoV-2 RNAs with an optofluidic nanopore sensor. Biosens. Bioelectron. 194, 113588.
Shawky, S.M., Awad, A.M., Allam, W., Alkordi, M.H., El-Khamisy, S.F., 2017a. Gold aggregating gold: a novel nanoparticle biosensor approach for the direct quantification of hepatitis C virus RNA in clinical samples. Biosens. Bioelectron. 92, 349–356.
Shawky, S.M., Awad, A.M., Allam, W., Alkordi, M.H., El-Khamisy, S.F., 2017b. Gold aggregating gold: a novel nanoparticle biosensor approach for the direct quantification of hepatitis C virus RNA in clinical samples. Biosens. Bioelectron. 92, 349–356.
Sheta, S.M., El-Sheikh, S.M., Osman, D.I., Salem, A.M., Ali, O.I., Harraz, F.A., Shousha, W.G., Shoeib, M.A., Shawky, S.M., Dionysiou, D.D., 2020a. A novel HCV electrochemical biosensor based on a polyaniline@ Ni-MOF nanocomposite. Dalton Trans. 49, 8918–8926.
Sheta, S.M., El-Sheikh, S.M., Osman, D.I., Salem, A.M., Ali, O.I., Harraz, F.A., Shousha, W.G., Shoeib, M.A., Shawky, S.M., Dionysiou, D.D., 2020b. A novel HCV electrochemical biosensor based on a polyaniline@ Ni-MOF nanocomposite. Dalton Trans. 49, 8918–8926.
Singh, A.K., Mittal, S., Das, M., Saharia, A., Tiwari, M., 2023. Optical biosensors: a decade in review. Alex. Eng. J. 67, 673–691.
Tan, M., Liao, C., Liang, L., Yi, X., Zhou, Z., Wei, G., 2022. Recent advances in recombinase polymerase amplification: principle, advantages, disadvantages and applications. Front. Cell. Infect. Microbiol. 12, 1019071.
Thompson, D., Lei, Y., 2020. Mini review: recent progress in RT-LAMP enabled COVID-19 detection. Sensors and Actuators Reports, 100017.
Wang, Z., Dai, Z., 2015. Carbon nanomaterial-based electrochemical biosensors: an overview. Nanoscale 7, 6420–6431.

Wu, C.-C., Yen, H.-Y., Lai, L.-T., Perng, G.-C., Lee, C.-R., Wu, S.-J., 2020a. A label-free impedimetric genosensor for the nucleic acid amplification-free detection of extracted RNA of dengue virus. Sensors 20, 3728.
Wu, C.-C., Yen, H.-Y., Lai, L.-T., Perng, G.-C., Lee, C.-R., Wu, S.-J., 2020b. A label-free impedimetric genosensor for the nucleic acid amplification-free detection of extracted RNA of dengue virus. Sensors 20, 3728.
Wu, Y., Ji, D., Dai, C., Kong, D., Chen, Y., Wang, L., Guo, M., Liu, Y., Wei, D., 2022a. Triple-probe DNA framework-based transistor for SARS-CoV-2 10-in-1 pooled testing. Nano Lett. 22, 3307–3316.
Wu, Y., Ji, D., Dai, C., Kong, D., Chen, Y., Wang, L., Guo, M., Liu, Y., Wei, D., 2022b. Triple-probe DNA framework-based transistor for SARS-CoV-2 10-in-1 pooled testing. Nano Lett. 22, 3307–3316.
Yang, Z., Wang, N., Wen, H., Cui, R., Yu, J., Yang, S., Qu, T., Wang, X., He, S., Qi, J., 2019. An amplification-free detection method of nucleic acids by a molecular beacon probe based on endonuclease activity. Sensor. Actuator. B Chem. 298, 126901.
Yin, B., Zhang, Q., Xia, X., Li, C., Ho, W.K.H., Yan, J., Huang, Y., Wu, H., Wang, P., Yi, C., 2022. A CRISPR-Cas12a integrated SERS nanoplatform with chimeric DNA/RNA hairpin guide for ultrasensitive nucleic acid detection. Theranostics 12, 5914.
Yu, H., Zhang, H., Li, J., Zhao, Z., Deng, M., Ren, Z., Li, Z., Xue, C., Li, M.G., Chen, Z., 2022a. Rapid and unamplified detection of SARS-CoV-2 RNA via CRISPR-Cas13a-modified solution-gated graphene transistors. ACS Sens. 7, 3923–3932.
Yu, H., Zhang, H., Li, J., Zhao, Z., Deng, M., Ren, Z., Li, Z., Xue, C., Li, M.G., Chen, Z., 2022b. Rapid and unamplified detection of SARS-CoV-2 RNA via CRISPR-Cas13a-modified solution-gated graphene transistors. ACS Sens. 7, 3923–3932.
Zambry, N.S., Awang, M.S., Beh, K.K., Hamzah, H.H., Bustami, Y., Obande, G.A., Khalid, M.F., Ozsoz, M., Abd Manaf, A., Aziah, I., 2023a. A label-free electrochemical DNA biosensor used a printed circuit board gold electrode (PCBGE) to detect SARS-CoV-2 without amplification. Lab Chip 23, 1622–1636.
Zambry, N.S., Awang, M.S., Beh, K.K., Hamzah, H.H., Bustami, Y., Obande, G.A., Khalid, M.F., Ozsoz, M., Abd Manaf, A., Aziah, I., 2023b. A label-free electrochemical DNA biosensor used a printed circuit board gold electrode (PCBGE) to detect SARS-CoV-2 without amplification. Lab Chip 23, 1622–1636.
Zucolotto, V., Daghastanli, K.R.P., Hayasaka, C.O., Riul, A., Ciancaglini, P., Oliveira, O. N., 2007. Using capacitance measurements as the detection method in antigen-containing layer-by-layer films for biosensing. Anal. Chem. 79, 2163–2167.